

## Design, synthesis and biological evaluation of novel 4-anilinoquinazoline derivatives as EGFR inhibitors with the potential to inhibit the gefitinib-resistant nonsmall cell lung cancers

Caolin Wang\*, Shan Xu\*, Liang Peng, Bingliang Zhang, Hong Zhang, Yingying Hu, Pengwu Zheng and Wufu Zhu

Jiangxi Provincial Key Laboratory of Drug Design and Evaluation, School of Pharmacy, Jiangxi Science & Technology Normal University, Nanchang, Jiangxi, China

### ABSTRACT

A series of quinazoline derivatives with benzylidene hydrazine carboxamide were designed and synthesised as EGFR inhibitors. Most compounds exhibited exceptional anti-proliferative activity against A549, HepG2, MCF-7 and H1975 cells. Furthermore, six compounds demonstrated excellent inhibition activity against EGFR<sup>WT</sup> with the IC<sub>50</sub> value both less than 2 nM. Among the six compounds, **44** exhibited the strongest activity (0.4 nM) and potently inhibited EGFR<sup>L858R/T790M</sup> (0.1 μM). Excitingly, the most potent compound **14** showed excellent enzyme inhibitory activity with 6.3 nM and 8.4 nM for both EGFR<sup>WT</sup> and EGFR<sup>T790M/L858R</sup>. The result of AO single staining and Annexin V/PI staining showed that the compound **14** and **44** could induce remarkable apoptosis of A549 cells. The compound **14** arrested the cell cycle at the S phase and compound **44** arrested the cell cycle at the G<sub>0</sub> phase in A549 cells. These preliminary results demonstrate that compound **14** and **44** may be promising lead compound-targeting EGFR.

### ARTICLE HISTORY

Received 23 June 2018  
Revised 18 August 2018  
Accepted 28 August 2018

### KEYWORDS

Quinazoline derivatives;  
benzylidene hydrazine;  
NSCLC; EGFR; inhibitors

### Introduction

Epidermal growth factor receptor (EGFR) is overexpressed in several human tumours including non-small cell lung cancer (NSCLC)<sup>1</sup>. As a target of NSCLC treatment, EGFR has become a hotspot in anti-tumour research in past few years<sup>2–4</sup>. Some EGFR small molecule inhibitors have yielded good results in tumour targeted therapies. The first generation of EGFR inhibitors erlotinib and gefitinib (Figure 1) has achieved remarkable benefits in patients carrying “sensitizing mutations” such as L858R and exon-19 deletions<sup>5</sup>. Unfortunately, most patients develop resistance after 10–14 months of treatment with gefitinib and erlotinib, and the statistics show that gatekeeper residue (T790M) mutation was detected in 50%<sup>6,7</sup>.

For this mutation, covalent inhibitors were developed to overcome these resistances. Afatinib, a typical covalent inhibitor and an ATP-competitive anilinoquinazoline derivative, was approved by the US FDA in 2013 for advanced NSCLC patients with active mutant EGFR<sup>8</sup>. However, afatinib contains a reactive “warhead” which can irreversibly bind to proteins other than the target, resulting in a toxic burden that limits its clinical utility<sup>6,8,9</sup>. AZD9291, a third-generation irreversible inhibitor and approved by the FDA in November 2015 for the treatment of EGFR T790M mutation in NSCLC patients, has a 200-fold selectivity for the T790M/L858R double mutant over wild-type EGFR<sup>10</sup>. These inhibitors contain an electrophilic Michael addition receptor moiety that can covalently bind to the conserved cysteine residue (Cys797) of EGFR at the lip of the ATP binding cleft of EGFR to facilitate the occupation of the EGFR ATP binding site and overcome the resistance caused by the T790M<sup>11</sup>.

A recent study exposed the occurrence of the tertiary point mutation C797S in 40% of the patients treated with AZD9291<sup>12</sup>. This mutation causes the drug molecules to lose covalent interactions, thereby resulting in a decrease in inhibitory activity. These data indicated that there is a great need to solve the mutation problem without relying on covalent reaction with Cys797. Therefore, developing noncovalent inhibitors strategy to overcome the T790M mutation attracted the researchers’ attention<sup>13,14</sup>. Chen et al.<sup>15</sup> reported that compound **BMC2009069-9a** is a novel non-covalent inhibitors candidate with the potency to overcome the problem of T790M.

In our previous study, a series of quinazoline derivatives were designed and synthesised as noncovalent EGFR inhibitors<sup>16</sup>. The most promising compound **BMC201725-9o** exhibited inhibitory activity against EGFR (IC<sub>50</sub> = 56 nM). Further research shows that **BMC201725-9o** can induce apoptosis in A549 cells, but shows weak inhibitory activity against EGFR<sup>L858R/T790M</sup> (IC<sub>50</sub> > 1000 nM). In this study, in order to enhance the inhibitory activity of EGFR against L858R/T790M mutation and improve the target compounds properties, further structural modifications were mainly focused on the position C-7 of quinazoline. The goal of structural modification was to increase inhibitory activity against T790M by increasing the interaction of the compound with the ATP binding site and reduce oxidation of phenolic hydroxyl groups. Following this method, we synthesised one novel quinazoline derivatives by three modification strategies: (a) The introduction of a polar flexible chain on the oxygen atom allows the solubilised tail to better reach the solvent zone. (b) According to the principle of bio-electronic isosteres, oxygen atom is replaced by a more stable carbon

**CONTACT** Wufu Zhu  [zhuwufu-1122@163.com](mailto:zhuwufu-1122@163.com), [zhuwf@jxstnu.edu.cn](mailto:zhuwf@jxstnu.edu.cn); Pengwu Zheng  [zhengpw@126.com](mailto:zhengpw@126.com)  Jiangxi Provincial Key Laboratory of Drug Design and Evaluation, School of Pharmacy, Jiangxi Science & Technology Normal University, 605 Fenglin Road, Nanchang, Jiangxi 330013, China

\*These authors contribute equally to this work.

 Supplemental data for this article can be accessed [here](#).

© 2018 The Author(s). Published by Informa UK Limited, trading as Taylor & Francis Group.

This is an Open Access article distributed under the terms of the Creative Commons Attribution-NonCommercial License (<http://creativecommons.org/licenses/by-nc/4.0/>), which permits unrestricted non-commercial use, distribution, and reproduction in any medium, provided the original work is properly cited.

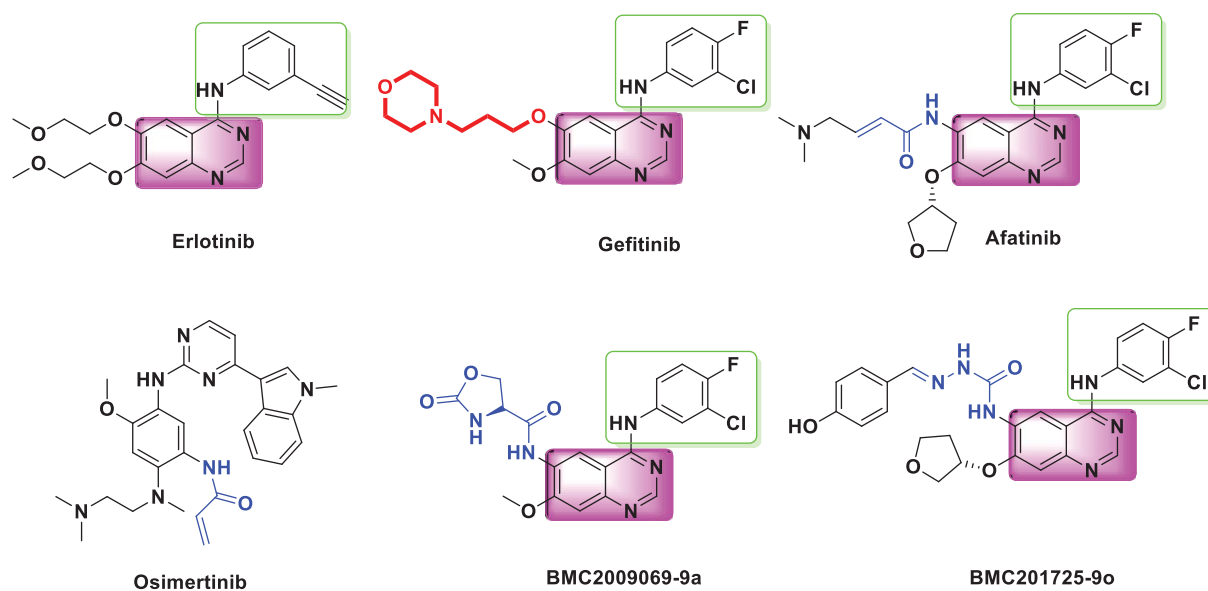


Figure 1. The chemical structures of several small molecule EGFR inhibitors.

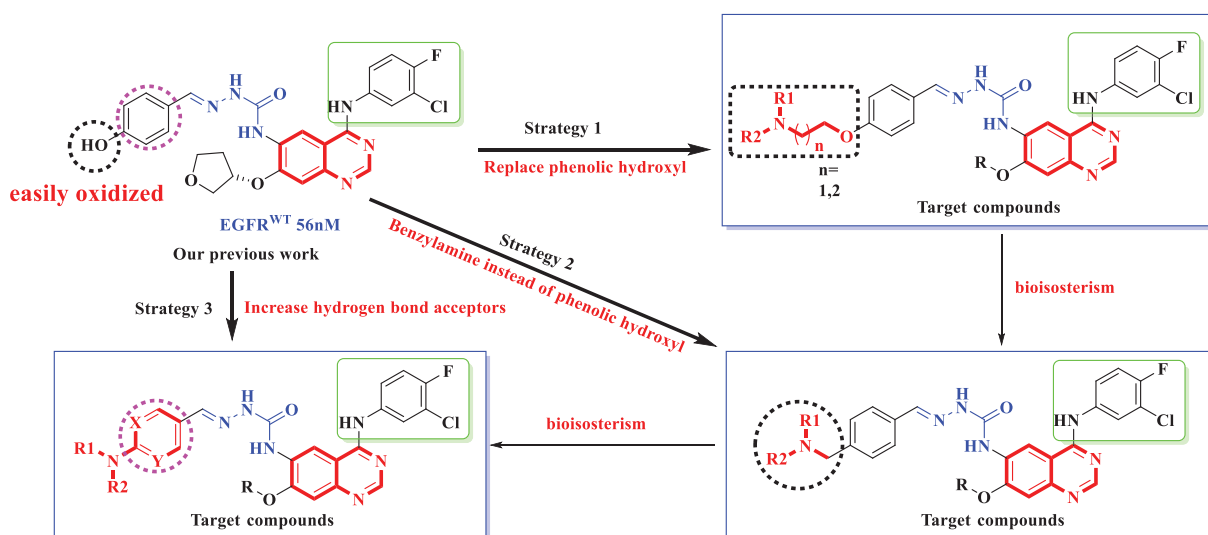


Figure 2. Structures and design strategy for target compounds 9–54.

atom. (c) Adding heteroatoms on benzene rings to increase hydrogen bonding receptors. The design strategy is shown in Figure 2.

Herein we assessed antitumour activity of all target compounds against A549, HepG2, MCF-7, H1975 cancer cell lines. In addition, the EGFR<sup>WT</sup> and EGFR<sup>L858R/T790M</sup> kinase inhibitory activities of some potential compounds were evaluated. Among these designed compounds, compounds 14 and 44 showed the potential against cell and mutant EGFR kinases, which was demonstrated the potential for overcoming the T790M mutant. In addition, this article further disclosed studies data on docking studies, AO single staining, cell cycle and apoptosis of 14 and 44.

## Materials and methods

### Reagents and general methods

All reagents and solvents used were purchased from commercial sources without further purification. Flash chromatography was performed using silica gel (200–300 mesh). All reactions were monitored by TLC, using silica gel plates with fluorescence F254

and UV light visualisation. <sup>1</sup>H NMR and <sup>13</sup>C NMR spectra were recorded on a Bruker AV-400 spectrometer at 400 MHz and Bruker AV-500 spectrometer at 125 MHz using deuterated solvents as an internal standard. Coupling constants (J) are expressed in hertz (Hz). Chemical shifts (δ) are given in parts per million (ppm). High-resolution ESI-MS were recorded on an Applied Biosystems Q-STAR Elite ESI- LC- MS/MS mass spectrometer. The purity of compounds was determined with reverse-phase HPLC analysis to be over 95% (see Supporting information). HPLC instrument: Dionex Summit HPLC (Column: Diamonsil C18, 5.0 mm, 4.6 250 mm (Agilent Technologies); detector: PDA-100 photodiode array; injector: ASI-100 autoinjector; pump: p-680A). A flow rate of 1.0 ml/min was used with mobile phase of MeOH in H<sub>2</sub>O with 0.1% modifier (ammonia v/v).

### Preparation of compounds 1–6

Compounds 1–6 were synthesised according to the procedures in our previous journal research<sup>16</sup>.

**Preparation of (S)-phenyl (4-((3-chloro-4-fluorophenyl)amino)-7-((tetrahydrofuran-3-yl)oxy)quinazolin-6-yl) carbamate (7a).** To the mixture of phenyl chloroformate (13.8 g, 88.5 mmol) and DIPEA (11.5 g, 88.5 mmol) in anhydrous 1,4-dioxane (80 ml), a solution of compound **6a** (13.5 g, 35.4 mmol) in anhydrous 1,4-dioxane (60 ml) was slowly added at 10 °C. After the addition was completed, the mixture was warmed to room temperature for another 1.5 h, and the solvent was evaporated under reduced pressure. The residue was dissolved in dichloromethane (60 ml), and washed with water (3 × 20 ml), dried over anhydrous Na<sub>2</sub>SO<sub>4</sub>, concentrated under reduced pressure to afford (S)-phenyl(4-((3-chloro-4-fluorophenyl)amino)-7-((tetrahydrofuran-3-yl)oxy)quinazolin-6-yl) carbamate **7a** as yellow oil (15.8 g, 90.3%), which were immediately used in the next step without further purification. ESI-MS m/z: [M + H]<sup>+</sup> 496.1.

**Preparation of phenyl (4-((3-chloro-4-fluorophenyl) amino)-7-methoxy quinazolin-6-yl)carbamate (7b).** To the mixture of phenyl chloroformate (13.8 g, 88.5 mmol) and DIPEA (11.5 g, 88.5 mmol) in anhydrous 1,4-dioxane (60 ml), a solution of compound **6b** (11.3 g, 35.4 mmol) in anhydrous 1,4-dioxane (30 ml) was slowly added at 10 °C. After the addition was completed, the mixture was warmed to room temperature for another 1.5 h, and the solution was poured into water with stirring for 15 min. The precipitate was filtered and washed with water, dried to furnish phenyl (4-((3-chloro-4-fluorophenyl) amino)-7-methoxy quinazolin-6-yl) carbamate **7b** as light yellow solid (14.2 g, 91.6%)<sup>14</sup>, which were immediately used in the next step without further purification. ESI-MS m/z: [M + H]<sup>+</sup> 439.1. <sup>1</sup>H NMR (400 MHz, DMSO-*d*<sub>6</sub>) δ 9.36 (d, *J* = 14.2 Hz, 2H), 8.37 (s, 1H), 8.18 (d, *J* = 5.0 Hz, 1H), 7.86–7.74 (m, 1H), 7.38 (d, *J* = 4.2 Hz, 2H), 7.15 (s, 2H), 7.10 (s, 1H), 6.75 (d, *J* = 7.7 Hz, 3H), 3.96 (s, 3H).

**Preparation of N-(4-((3-chloro-4-fluorophenyl)amino)-7-(cyclopentyl)oxy)quinazolin-6-yl) hydrazinecarboxamide (8a).** A mixture of **7a** (4.2 g, 8.40 mmol) and 80% hydrazine monohydrate (3 ml) in 1,4-dioxane (20 ml) was refluxed for 2 h and monitored by TLC. After cooling to room temperature, the yellow solid was filtered off and washed with 1,4-dioxane and water, and dried to afford the (S)-N-(4-((3-chloro-4-fluorophenyl)amino)-7-((tetrahydrofuran-3-yl)oxy)quinazolin-6-yl)hydrazine carboxamide **8a** as a white solid (2.4 g, 65.2%)<sup>16</sup>. Mp 262.3–263.7 °C. ESI-MS m/z: [M + H]<sup>+</sup> 434.1. <sup>1</sup>H NMR (400 MHz, DMSO-*d*<sub>6</sub>) δ 9.78 (s, 1H), 9.28 (s, 1H), 8.92 (s, 1H), 8.43 (d, *J* = 12.7 Hz, 1H), 8.07 (d, *J* = 6.6 Hz, 1H), 7.92 (s, 1H), 7.76 (d, *J* = 8.6 Hz, 1H), 7.40 (t, *J* = 9.1 Hz, 1H), 7.24 (s, 1H), 5.36 (s, 1H), 4.68 (s, 2H), 4.01 (dd, *J* = 10.2, 4.0 Hz, 1H), 3.98–3.86 (m, 2H), 3.82 (dd, *J* = 12.4, 7.9 Hz, 1H), 2.37 (td, *J* = 12.2, 7.5 Hz, 1H), 2.15–1.84 (m, 1H).

**N-(4-((3-chloro-4-fluorophenyl)amino)-7-methoxy quinazolin-6-yl)hydrazine carboxamide (8b).** The synthesis of compound **8b** was similar to the compound **8a**. A mixture of **7b** (4.0 g, 9.12 mmol) and 80% hydrazine monohydrate (5 ml) in 1,4-dioxane (20 ml) was refluxed for 2 h and monitored by TLC. After cooling to room temperature, the white solid was filtered off and washed with water, and dried to afford the N-(4-((3-chloro-4-fluorophenyl)amino)-7-methoxy quinazolin-6-yl) hydrazine carboxamide **8b** as a white solid (2.4 g, 68.5%) [16]. Mp 263.8–264.6 °C. ESI-MS m/z: [M + H]<sup>+</sup> 376.1. <sup>1</sup>H NMR (400 MHz, DMSO-*d*<sub>6</sub>) δ 9.76 (s, 1H), 9.20 (s, 1H), 8.91 (s, 1H), 8.47 (s, 1H), 8.07 (d, *J* = 4.9 Hz, 1H), 7.90 (s, 1H), 7.81–7.69 (m, 1H), 7.40 (t, *J* = 9.1 Hz, 1H), 7.27 (s, 1H), 4.67 (s, 2H), 4.04 (s, 3H).

#### General procedure for the preparation of compounds 9–54

To a solution of **8a–b** (0.46 mmol) in Ethanol/DMF (4 ml), 1.1 equiv of aldehydes and 98% sulfuric acid (1 drop) were added, and the

mixture was refluxed for 9–10 h until TLC showed the completion of the reaction. After cooling to room temperature, the precipitate was filtered and dried to yield **9–54** which were purified by isopropanol<sup>16</sup>.

**(E)-N-(4-((3-chloro-4-fluorophenyl)amino)-7-methoxyquinazolin-6-yl)-2-(4-(dimethylamino)benzylidene)hydrazine-1-carboxamide (9).** This compound was obtained as white solid in 88% yield. Mp 236.4–239.4 °C. ESI-MS m/z: [M + H]<sup>+</sup> 507.1. <sup>1</sup>H NMR (400 MHz, DMSO-*d*<sub>6</sub>) δ 10.84 (s, 1H), 9.83 (s, 1H), 9.07 (s, 1H), 8.92 (d, *J* = 8.4 Hz, 1H), 8.51 (s, 1H), 8.10 (d, *J* = 6.6 Hz, 1H), 7.88 (d, *J* = 11.7 Hz, 1H), 7.79 (s, 1H), 7.53 (d, *J* = 8.7 Hz, 2H), 7.46–7.37 (m, 1H), 7.32 (s, 1H), 6.79 (d, *J* = 8.5 Hz, 2H), 4.13 (s, 3H), 2.98 (s, 6H).

**(S,E)-N-(4-((3-chloro-4-fluorophenyl)amino)-7-((tetrahydrofuran-3-yl)oxy)quinazolin-6-yl)-2-(4-(dimethylamino)benzylidene)hydrazine-1-carboxamide (10).** This compound was obtained as yellow solid in 76% yield. Mp 238.4–241.2 °C. ESI-MS m/z: [M + H]<sup>+</sup> 563.1. <sup>1</sup>H NMR (400 MHz, DMSO-*d*<sub>6</sub>) δ 10.89 (s, 1H), 9.86 (s, 1H), 9.13 (s, 1H), 9.00 (s, 1H), 8.50 (s, 1H), 8.08 (d, *J* = 6.1 Hz, 1H), 7.89 (s, 1H), 7.78 (s, 1H), 7.54 (d, *J* = 8.1 Hz, 2H), 7.41 (t, *J* = 9.0 Hz, 1H), 7.32 (s, 1H), 6.73 (d, *J* = 8.3 Hz, 2H), 5.45 (s, 1H), 4.04 (s, 2H), 4.01–3.95 (m, 1H), 3.89 (d, *J* = 4.5 Hz, 1H), 2.98 (s, 6H), 2.43 (dd, *J* = 13.8, 6.7 Hz, 1H), 2.18 (s, 1H).

**(E)-N-(4-((3-chloro-4-fluorophenyl)amino)-7-methoxyquinazolin-6-yl)-2-(4-(diethylamino)benzylidene)hydrazine-1-carboxamide (11).** This compound was obtained as white solid in 86% yield. Mp 226.1–229.4 °C. ESI-MS m/z: [M + H]<sup>+</sup> 535.1. <sup>1</sup>H NMR (400 MHz, DMSO-*d*<sub>6</sub>) δ 10.84 (s, 1H), 9.83 (s, 1H), 9.07 (s, 1H), 8.92 (d, *J* = 8.4 Hz, 1H), 8.51 (s, 1H), 8.10 (d, *J* = 6.6 Hz, 1H), 7.88 (d, *J* = 11.7 Hz, 1H), 7.79 (s, 1H), 7.53 (d, *J* = 8.7 Hz, 2H), 7.46–7.37 (m, 1H), 7.32 (s, 1H), 6.79 (d, *J* = 8.5 Hz, 2H), 4.13 (s, 3H), 2.98 (s, 6H).

**(S,E)-N-(4-((3-chloro-4-fluorophenyl)amino)-7-((tetrahydrofuran-3-yl)oxy)quinazolin-6-yl)-2-(4-(diethylamino)benzylidene)hydrazine-1-carboxamide (12).** This compound was obtained as white solid in 84% yield. Mp 236.4–238.9 °C. ESI-MS m/z: [M + H]<sup>+</sup> 591.2. <sup>1</sup>H NMR (400 MHz, DMSO) δ 10.85 (dd, *J* = 48.5, 28.5 Hz, 1H), 10.13–9.58 (m, 1H), 9.09 (s, 1H), 8.98 (s, 1H), 8.40 (s, 1H), 8.02 (s, 1H), 7.87 (s, 1H), 7.68 (s, 1H), 7.51 (d, *J* = 8.7 Hz, 2H), 7.36 (s, 1H), 7.24 (s, 1H), 6.68 (d, *J* = 8.8 Hz, 2H), 5.42 (s, 1H), 4.05 (dt, *J* = 15.6, 6.6 Hz, 2H), 4.00–3.94 (m, 1H), 3.88 (dt, *J* = 12.7, 6.4 Hz, 1H), 3.40 (s, 4H), 2.42 (dd, *J* = 13.9, 6.2 Hz, 1H), 2.22–2.12 (m, 1H), 1.12 (t, *J* = 6.9 Hz, 6H).

**(S,E)-N-(4-((3-chloro-4-fluorophenyl)amino)-7-((tetrahydrofuran-3-yl)oxy)quinazolin-6-yl)-2-((5-morpholinothiazol-2-yl)methylene)hydrazine-1-carboxamide (13).** This compound was obtained as white solid in 86% yield. Mp 236.4–238.9 °C. ESI-MS m/z: [M + H]<sup>+</sup> 612.1. <sup>1</sup>H NMR (400 MHz, DMSO-*d*<sub>6</sub>) δ 11.04 (s, 1H), 9.85 (s, 1H), 9.02 (s, 1H), 8.86 (s, 1H), 8.50 (s, 1H), 8.08 (d, *J* = 6.8 Hz, 2H), 7.77 (dt, *J* = 7.4, 3.5 Hz, 1H), 7.58 (s, 1H), 7.42 (t, *J* = 9.1 Hz, 1H), 7.30 (s, 1H), 5.43 (s, 1H), 4.15–4.05 (m, 2H), 3.96 (q, *J* = 8.0 Hz, 1H), 3.88 (td, *J* = 8.2, 4.2 Hz, 1H), 3.74 (t, *J* = 4.9 Hz, 4H), 3.51 (t, *J* = 4.9 Hz, 4H), 2.40 (dt, *J* = 14.4, 7.1 Hz, 1H), 2.25–2.14 (m, 1H).

**(S,E)-N-(4-((3-chloro-4-fluorophenyl)amino)-7-((tetrahydrofuran-3-yl)oxy)quinazolin-6-yl)-2-((2-(pyrrolidin-1-yl)pyrimidin-5-yl)methylene)hydrazine-1-carboxamide (14).** This compound was obtained as yellow solid in 85% yield. Mp 236.4–238.9 °C. ESI-MS m/z: [M + H]<sup>+</sup> 591.1. <sup>1</sup>H NMR (400 MHz, DMSO-*d*<sub>6</sub>) δ 11.09 (s, 1H), 10.05 (s, 1H), 9.01 (s, 2H), 8.66 (s, 2H), 8.55 (s, 1H), 8.08 (dd, *J* = 6.8, 2.6 Hz, 1H), 7.89 (s, 1H), 7.77 (dd, *J* = 8.8, 4.0 Hz, 1H), 7.44 (t, *J* = 9.1 Hz, 1H), 7.32 (s, 1H), 5.43 (d, *J* = 5.3 Hz, 1H), 4.02 (dd, *J* = 10.1, 3.8 Hz, 2H), 3.98 (d, *J* = 9.2 Hz, 1H), 3.82 (dt, *J* = 8.4, 4.1 Hz, 1H), 3.56–3.52 (m, 4H), 2.47–2.39 (m, 1H), 2.16 (dd, *J* = 13.1, 6.4 Hz, 1H), 1.99–1.93 (m, 4H).

**(S,E)-N-(4-((3-chloro-4-fluorophenyl)amino)-7-((tetrahydrofuran-3-yl)oxy)quinazolin-6-yl)-2-((5-(pyrrolidin-1-yl)furan-2-yl)methylene)hydrazine-1-carboxamide (15).** This compound was obtained as

yellow solid in 78% yield. Mp 236.4–238.9 °C. ESI-MS  $m/z$ :  $[M + H]^+$  579.1.  $^1H$  NMR (400 MHz, DMSO)  $\delta$  11.07 (s, 1H), 10.06 (s, 1H), 9.09 (s, 1H), 8.65 (s, 1H), 8.55 (s, 1H), 8.08 (dd,  $J=6.8, 2.6$  Hz, 1H), 7.89 (s, 1H), 7.77 (dd,  $J=8.8, 4.0$  Hz, 1H), 7.44 (t,  $J=9.1$  Hz, 1H), 7.32 (s, 1H), 7.01 (s, 1H), 6.41 (s, 1H), 5.43 (d,  $J=5.3$  Hz, 1H), 4.02 (dd,  $J=10.1, 3.8$  Hz, 2H), 3.98 (d,  $J=9.2$  Hz, 1H), 3.82 (dt,  $J=8.4, 4.1$  Hz, 1H), 3.42–3.62 (m, 4H), 2.47–2.39 (m, 1H), 2.16 (dd,  $J=13.1, 6.4$  Hz, 1H), 1.93–1.89 (m, 4H).

(*S,E*)-*N*-(4-((3-chloro-4-fluorophenyl)amino)-7-((tetrahydrofuran-3-yl)oxy)quinazolin-6-yl)-2-((5-(dimethylamino)thiophen-2-yl)methylene)hydrazine-1-carboxamide (**16**). This compound was obtained as white solid in 89% yield. Mp 236.4–238.9 °C. ESI-MS  $m/z$ :  $[M + H]^+$  569.1.  $^1H$  NMR (400 MHz, DMSO- $d_6$ )  $\delta$  10.78 (s, 1H), 9.84 (s, 1H), 9.03 (s, 1H), 8.89 (s, 1H), 8.49 (s, 1H), 8.09 (s, 1H), 7.98 (s, 1H), 7.78 (s, 1H), 7.40 (d,  $J=9.1$  Hz, 1H), 7.29 (s, 1H), 7.10 (s, 1H), 5.88 (s, 1H), 5.41 (s, 1H), 4.10 (s, 2H), 3.99 (s, 1H), 3.86 (s, 1H), 2.99 (d,  $J=9.6$  Hz, 6H), 2.44–2.36 (m, 1H), 2.28–2.18 (m, 1H).

(*E*)-*N*-(4-((3-chloro-4-fluorophenyl)amino)-7-methoxyquinazolin-6-yl)-2-((6-(pyrrolidin-1-yl)pyridin-3-yl)methylene)hydrazine-1-carboxamide (**17**). This compound was obtained as yellow solid in 77% yield. Mp 236.4–238.9 °C. ESI-MS  $m/z$ :  $[M + H]^+$  534.1.  $^1H$  NMR (400 MHz, DMSO- $d_6$ )  $\delta$  10.87 (s, 1H), 9.81 (s, 1H), 9.00 (s, 1H), 8.90 (s, 1H), 8.50 (s, 1H), 8.24 (s, 1H), 8.09 (s, 1H), 7.89 (s, 2H), 7.78 (s, 1H), 7.45–7.36 (m, 1H), 7.30 (s, 1H), 6.59 (d,  $J=9.1$  Hz, 1H), 4.10 (d,  $J=4.9$  Hz, 3H), 3.43 (s, 4H), 1.95 (s, 4H).

(*S,E*)-*N*-(4-((3-chloro-4-fluorophenyl)amino)-7-((tetrahydrofuran-3-yl)oxy)quinazolin-6-yl)-2-((6-(pyrrolidin-1-yl)pyridin-3-yl)methylene)hydrazine-1-carboxamide (**18**). This compound was obtained as white solid in 79% yield. Mp 236.4–238.9 °C. ESI-MS  $m/z$ :  $[M + H]^+$  590.2.  $^1H$  NMR (400 MHz, DMSO- $d_6$ )  $\delta$  10.95 (s, 1H), 9.84 (s, 1H), 9.08 (s, 1H), 8.99 (s, 1H), 8.50 (s, 1H), 8.23 (d,  $J=2.1$  Hz, 1H), 8.09 (dd,  $J=6.9, 2.6$  Hz, 1H), 7.94 (d,  $J=9.8$  Hz, 1H), 7.90 (s, 1H), 7.80–7.75 (m, 1H), 7.41 (t,  $J=9.0$  Hz, 1H), 7.31 (s, 1H), 6.50 (d,  $J=8.8$  Hz, 1H), 5.44 (s, 1H), 4.02 (d,  $J=3.2$  Hz, 2H), 4.00–3.93 (m, 1H), 3.86 (d,  $J=5.0$  Hz, 1H), 3.44 (s, 4H), 2.46–2.36 (m, 1H), 2.20–2.11 (m, 1H), 1.96 (s, 4H).

(*E*)-*N*-(4-((3-chloro-4-fluorophenyl)amino)-7-methoxyquinazolin-6-yl)-2-4-((dimethylamino)methyl)benzylidene)hydrazine-1-carboxamide (**19**). This compound was obtained as white solid in 84% yield. Mp 226.5–229.4 °C. ESI-MS  $m/z$ :  $[M + H]^+$  521.1.  $^1H$  NMR (400 MHz, DMSO- $d_6$ )  $\delta$  11.12 (s, 1H), 9.84 (s, 1H), 9.08 (s, 1H), 8.92 (s, 1H), 8.52 (s, 1H), 8.11 (d,  $J=6.7$  Hz, 1H), 8.02 (s, 1H), 7.78 (s, 1H), 7.68 (d,  $J=7.8$  Hz, 2H), 7.40 (d,  $J=7.2$  Hz, 3H), 7.33 (s, 1H), 4.12 (s, 3H), 3.42 (s, 2H), 2.16 (s, 6H).

(*E*)-*N*-(4-((3-chloro-4-fluorophenyl)amino)-7-methoxyquinazolin-6-yl)-2-4-((diethylamino)methyl)benzylidene)hydrazine-1-carboxamide (**20**). This compound was obtained as white solid in 86% yield. Mp 226.1–229.6 °C. ESI-MS  $m/z$ :  $[M + H]^+$  549.2.  $^1H$  NMR (400 MHz, DMSO- $d_6$ )  $\delta$  11.12 (s, 1H), 9.84 (s, 1H), 9.08 (s, 1H), 8.92 (s, 1H), 8.52 (s, 1H), 8.11 (d,  $J=6.7$  Hz, 1H), 8.02 (s, 1H), 7.78 (s, 1H), 7.68 (d,  $J=7.8$  Hz, 2H), 7.40 (d,  $J=7.2$  Hz, 3H), 7.33 (s, 1H), 4.12 (s, 3H), 3.42 (s, 2H), 2.46–2.54 (m, 4H), 1.46 (s, 6H).

(*E*)-*N*-(4-((3-chloro-4-fluorophenyl)amino)-7-methoxyquinazolin-6-yl)-2-4-(pyrrolidin-1-ylmethyl)benzylidene)hydrazine-1-carboxamide (**21**). This compound was obtained as yellow solid in 89% yield. Mp 231.4–234.5 °C. ESI-MS  $m/z$ :  $[M + H]^+$  547.1.  $^1H$  NMR (400 MHz, DMSO- $d_6$ )  $\delta$  11.13 (s, 1H), 9.85 (s, 1H), 9.08 (s, 1H), 8.93 (s, 1H), 8.52 (s, 1H), 8.10 (s, 1H), 8.01 (s, 1H), 7.79 (s, 1H), 7.67 (d,  $J=8.2$  Hz, 2H), 7.42 (s, 3H), 7.33 (s, 1H), 4.12 (s, 3H), 3.60 (s, 2H), 2.44 (s, 4H), 1.70 (s, 4H).

(*E*)-*N*-(4-((3-chloro-4-fluorophenyl)amino)-7-methoxyquinazolin-6-yl)-2-4-(piperidin-1-ylmethyl)benzylidene)hydrazine-1-carboxamide (**22**). This compound was obtained as yellow solid in 92%

yield. Mp 235.4–237.5 °C. ESI-MS  $m/z$ :  $[M + H]^+$  561.2.  $^1H$  NMR (400 MHz, DMSO- $d_6$ )  $\delta$  11.14 (s, 1H), 9.86 (s, 1H), 9.08 (s, 1H), 8.93 (s, 1H), 8.53 (s, 1H), 8.10 (s, 1H), 8.02 (s, 1H), 7.79 (s, 1H), 7.68 (d,  $J=7.8$  Hz, 2H), 7.43 (s, 1H), 7.40 (s, 1H), 7.34 (s, 2H), 4.13 (d,  $J=2.3$  Hz, 3H), 3.46 (s, 2H), 2.34 (s, 4H), 1.51 (s, 4H), 1.40 (s, 2H).

(*E*)-*N*-(4-((3-chloro-4-fluorophenyl)amino)-7-methoxyquinazolin-6-yl)-2-4-(morpholinomethyl)benzylidene)hydrazine-1-carboxamide (**23**). This compound was obtained as white solid in 87% yield. Mp 236.4–239.5 °C. ESI-MS  $m/z$ :  $[M + H]^+$  563.1.  $^1H$  NMR (400 MHz, DMSO- $d_6$ )  $\delta$  11.15 (s, 1H), 9.87 (s, 1H), 9.10 (s, 1H), 8.93 (s, 1H), 8.56 (s, 1H), 8.12 (s, 1H), 8.03 (s, 1H), 7.80 (s, 1H), 7.78 (d,  $J=7.8$  Hz, 2H), 7.42 (s, 3H), 7.35 (s, 1H), 4.13 (d,  $J=2.3$  Hz, 3H), 3.66 (s, 2H), 3.45 (s, 4H), 2.44 (s, 4H).

(*E*)-*N*-(4-((3-chloro-4-fluorophenyl)amino)-7-methoxyquinazolin-6-yl)-2-4-((4-methylpiperazin-1-yl)methyl)benzylidene)hydrazine-1-carboxamide (**24**). This compound was obtained as yellow solid in 81% yield. Mp 231.4–235.8 °C. ESI-MS  $m/z$ :  $[M + H]^+$  576.2.  $^1H$  NMR (400 MHz, DMSO- $d_6$ )  $\delta$  11.12 (s, 1H), 9.84 (s, 1H), 9.07 (s, 1H), 8.93 (s, 1H), 8.52 (s, 1H), 8.11 (s, 1H), 8.01 (s, 1H), 7.80 (s, 1H), 7.68 (d,  $J=8.2$  Hz, 2H), 7.44 (s, 1H), 7.41 (d,  $J=7.5$  Hz, 2H), 7.34 (s, 1H), 4.09 (d,  $J=26.9$  Hz, 3H), 3.49 (s, 2H), 2.53 (s, 4H), 2.39–2.30 (m, 4H), 2.15 (s, 3H).

(*S,E*)-*N*-(4-((3-chloro-4-fluorophenyl)amino)-7-((tetrahydrofuran-3-yl)oxy)quinazolin-6-yl)-2-4-((dimethylamino)methyl)benzylidene)hydrazine-1-carboxamide (**25**). This compound was obtained as white solid in 86% yield. Mp 236.4–239.5 °C. ESI-MS  $m/z$ :  $[M + H]^+$  577.2.  $^1H$  NMR (400 MHz, DMSO- $d_6$ )  $\delta$  11.19 (s, 1H), 9.86 (s, 1H), 9.15 (s, 1H), 9.01 (s, 1H), 8.51 (s, 1H), 8.09 (dd,  $J=6.9, 2.6$  Hz, 1H), 8.02 (s, 1H), 7.80–7.75 (m, 1H), 7.69 (d,  $J=7.9$  Hz, 2H), 7.40 (d,  $J=9.1$  Hz, 1H), 7.37 (s, 1H), 7.34 (d,  $J=6.3$  Hz, 2H), 5.45 (s, 1H), 4.05 (d,  $J=3.3$  Hz, 2H), 3.97 (q,  $J=7.7$  Hz, 1H), 3.91–3.83 (m, 1H), 3.41 (s, 2H), 2.47–2.39 (m, 1H), 2.18 (d,  $J=6.7$  Hz, 1H), 2.1 (s, 6H).

(*S,E*)-*N*-(4-((3-chloro-4-fluorophenyl)amino)-7-((tetrahydrofuran-3-yl)oxy)quinazolin-6-yl)-2-4-((diethylamino)methyl)benzylidene)hydrazine-1-carboxamide (**26**).

This compound was obtained as yellow solid in 81% yield. Mp 226.4–231.5 °C. ESI-MS  $m/z$ :  $[M + H]^+$  605.2.  $^1H$  NMR (400 MHz, DMSO- $d_6$ )  $\delta$  11.19 (s, 1H), 9.86 (s, 1H), 9.15 (s, 1H), 9.01 (s, 1H), 8.51 (s, 1H), 8.09 (dd,  $J=6.9, 2.6$  Hz, 1H), 8.02 (s, 1H), 7.80–7.75 (m, 1H), 7.69 (d,  $J=7.9$  Hz, 2H), 7.40 (d,  $J=9.1$  Hz, 1H), 7.37 (s, 1H), 7.34 (d,  $J=6.3$  Hz, 2H), 5.45 (s, 1H), 4.05 (d,  $J=3.3$  Hz, 2H), 3.97 (q,  $J=7.7$  Hz, 1H), 3.91–3.83 (m, 1H), 3.41 (s, 2H), 2.54 (s, 4H), 2.47–2.39 (m, 1H), 2.18 (d,  $J=6.7$  Hz, 1H), 1.51 (s, 6H).

(*S,E*)-*N*-(4-((3-chloro-4-fluorophenyl)amino)-7-((tetrahydrofuran-3-yl)oxy)quinazolin-6-yl)-2-4-(pyrrolidin-1-ylmethyl)benzylidene)hydrazine-1-carboxamide (**27**). This compound was obtained as white solid in 83% yield. Mp 235.4–239.5 °C. ESI-MS  $m/z$ :  $[M + H]^+$  603.2.  $^1H$  NMR (400 MHz, DMSO- $d_6$ )  $\delta$  11.18 (s, 1H), 9.86 (s, 1H), 9.14 (s, 1H), 9.01 (s, 1H), 8.50 (s, 1H), 8.09 (s, 1H), 8.01 (s, 1H), 7.78 (s, 1H), 7.67 (d,  $J=7.8$  Hz, 2H), 7.38 (dt,  $J=21.0, 11.0$  Hz, 4H), 5.45 (s, 1H), 4.05 (s, 2H), 3.97 (d,  $J=7.3$  Hz, 1H), 3.87 (s, 1H), 3.59 (s, 2H), 2.49 (s, 1H), 2.43 (s, 4H), 2.17 (s, 1H), 1.70 (s, 4H).

(*S,E*)-*N*-(4-((3-chloro-4-fluorophenyl)amino)-7-((tetrahydrofuran-3-yl)oxy)quinazolin-6-yl)-2-4-(piperidin-1-ylmethyl)benzylidene)hydrazine-1-carboxamide (**28**). This compound was obtained as yellow solid in 87% yield. Mp 236.4–238.5 °C. ESI-MS  $m/z$ :  $[M + H]^+$  617.2.  $^1H$  NMR (400 MHz, DMSO- $d_6$ )  $\delta$  11.16 (s, 1H), 9.85 (s, 1H), 9.13 (s, 1H), 9.00 (s, 1H), 8.49 (s, 1H), 8.07 (d,  $J=4.4$  Hz, 1H), 8.00 (s, 1H), 7.75 (s, 1H), 7.66 (d,  $J=8.0$  Hz, 2H), 7.43–7.31 (m, 4H), 5.43 (s, 1H), 4.04 (s, 2H), 3.95 (dd,  $J=15.7, 7.9$  Hz, 1H), 3.85 (dd,  $J=13.1, 8.3$  Hz, 1H), 3.44 (s, 2H), 2.40 (dd,  $J=14.1, 8.0$  Hz, 1H), 2.31 (s, 4H), 2.19–2.10 (m, 1H), 1.48 (d,  $J=5.2$  Hz, 4H), 1.38 (s, 2H).

(*S,E*)-*N*-(4-((3-chloro-4-fluorophenyl)amino)-7-((tetrahydrofuran-3-yl)oxy)quinazolin-6-yl)-2-(4-(morpholinomethyl)benzylidene)hydrazine-1-carboxamide (**29**). This compound was obtained as white solid in 86% yield. Mp 232.4–236.8 °C. ESI-MS *m/z*: [M + H]<sup>+</sup> 619.2. <sup>1</sup>H NMR (400 MHz, DMSO-*d*<sub>6</sub>) δ 11.28 (s, 1H), 9.97 (s, 1H), 9.24 (s, 1H), 9.11 (s, 1H), 8.60 (s, 1H), 8.18 (d, *J* = 4.7 Hz, 1H), 8.11 (s, 1H), 7.87 (d, *J* = 7.8 Hz, 1H), 7.77 (d, *J* = 7.9 Hz, 2H), 7.47 (dd, *J* = 20.2, 12.3 Hz, 4H), 5.55 (s, 1H), 4.15 (s, 2H), 4.08–4.03 (m, 1H), 3.99–3.93 (m, 1H), 3.69 (s, 2H), 2.53 (s, 4H), 2.48 (d, *J* = 9.4 Hz, 1H), 2.30–2.18 (m, 1H), 1.80 (s, 4H).

(*S,E*)-*N*-(4-((3-chloro-4-fluorophenyl)amino)-7-((tetrahydrofuran-3-yl)oxy)quinazolin-6-yl)-2-(4-((4-methylpiperazin-1-yl)methyl)benzylidene)hydrazine-1-carboxamide (**30**). This compound was obtained as white solid in 85% yield. Mp 233.4–237.6 °C. ESI-MS *m/z*: [M + H]<sup>+</sup> 632.2. <sup>1</sup>H NMR (400 MHz, DMSO-*d*<sub>6</sub>) δ 11.28 (s, 1H), 9.97 (s, 1H), 9.24 (s, 1H), 9.11 (s, 1H), 8.60 (s, 1H), 8.18 (d, *J* = 4.7 Hz, 1H), 8.11 (s, 1H), 7.87 (d, *J* = 7.8 Hz, 1H), 7.77 (d, *J* = 7.9 Hz, 2H), 7.47 (dd, *J* = 20.2, 12.3 Hz, 4H), δ 5.36 (s, 1H), 4.03 (d, *J* = 3.3 Hz, 2H), 3.96 (d, *J* = 7.8 Hz, 1H), 3.86 (dd, *J* = 8.4, 4.7 Hz, 1H), 3.48 (s, 2H), 2.66–2.51 (m, 4H), 2.38 (s, 4H), 2.15 (s, 3H).

(*E*)-*N*-(4-((3-chloro-4-fluorophenyl)amino)-7-methoxyquinazolin-6-yl)-2-(4-(2-(dimethylamino)ethoxy)benzylidene)hydrazine-1-carboxamide (**31**). This compound was obtained as white solid in 76% yield. Mp 205.2–209.5 °C. ESI-MS *m/z*: [M + H]<sup>+</sup> 551.18. <sup>1</sup>H NMR (400 MHz, DMSO-*d*<sub>6</sub>) δ 10.98 (s, 1H), 9.80 (s, 1H), 9.02 (s, 1H), 8.88 (d, *J* = 4.0 Hz, 1H), 8.47 (d, *J* = 4.3 Hz, 1H), 8.06 (d, *J* = 4.2 Hz, 1H), 7.93 (d, *J* = 11.1 Hz, 1H), 7.74 (s, 1H), 7.61 (d, *J* = 8.5 Hz, 2H), 7.39 (d, *J* = 9.2 Hz, 1H), 7.27 (d, *J* = 9.0 Hz, 1H), 7.01 (d, *J* = 8.5 Hz, 2H), 4.07 (s, 3H), 4.06 (d, *J* = 5.3 Hz, 2H), 2.61 (d, *J* = 5.3 Hz, 2H), 2.18 (s, 6H).

(*E*)-*N*-(4-((3-chloro-4-fluorophenyl)amino)-7-methoxyquinazolin-6-yl)-2-(4-(2-(diethylamino)ethoxy)benzylidene)hydrazine-1-carboxamide (**32**). This compound was obtained as white solid in 79% yield. Mp 208.5–210.2 °C. ESI-MS *m/z*: [M + H]<sup>+</sup> 579.22. <sup>1</sup>H NMR (400 MHz, CDCl<sub>3</sub>) δ 11.01 (s, 1H), 9.84 (s, 1H), 9.06 (s, 1H), 8.92 (s, 1H), 8.51 (s, 1H), 8.09 (s, 1H), 7.96 (s, 1H), 7.78 (s, 1H), 7.65 (d, *J* = 8.3 Hz, 2H), 7.40 (d, *J* = 9.1 Hz, 1H), 7.32 (s, 1H), 7.04 (d, *J* = 8.9 Hz, 2H), 4.12 (s, 3H), 4.06 (d, *J* = 6.0 Hz, 2H), 2.78 (s, 2H), 2.55 (d, *J* = 7.0 Hz, 4H), 0.97 (t, *J* = 7.0 Hz, 6H).

(*E*)-*N*-(4-((3-chloro-4-fluorophenyl)amino)-7-methoxyquinazolin-6-yl)-2-(4-(2-(pyrrolidin-1-yl)ethoxy)benzylidene)hydrazine-1-carboxamide (**33**). This compound was obtained as yellow solid in 84% yield. Mp 203.2–208.8 °C. ESI-MS *m/z*: [M + H]<sup>+</sup> 577.2. <sup>1</sup>H NMR (400 MHz, DMSO-*d*<sub>6</sub>) δ 11.03 (s, 1H), 9.85 (s, 1H), 9.06 (s, 1H), 8.91 (s, 1H), 8.51 (s, 1H), 8.10 (dd, *J* = 7.0, 2.6 Hz, 1H), 7.96 (s, 1H), 7.78 (d, *J* = 8.9 Hz, 1H), 7.65 (d, *J* = 8.5 Hz, 2H), 7.42 (t, *J* = 9.2 Hz, 1H), 7.32 (s, 1H), 7.05 (d, *J* = 8.3 Hz, 2H), 4.12 (d, *J* = 6.7 Hz, 5H), 2.79 (d, *J* = 7.1 Hz, 2H), 2.52 (s, 4H), 1.68 (d, *J* = 5.5 Hz, 4H).

(*E*)-*N*-(4-((3-chloro-4-fluorophenyl)amino)-7-methoxyquinazolin-6-yl)-2-(4-(2-(piperidin-1-yl)ethoxy)benzylidene)hydrazine-1-carboxamide (**34**). This compound was obtained as white solid in 75% yield. Mp 205.6–208.4 °C. ESI-MS *m/z*: [M + H]<sup>+</sup> 591.22. <sup>1</sup>H NMR (400 MHz, DMSO-*d*<sub>6</sub>) δ 11.01 (s, 1H), 9.84 (s, 1H), 9.07 (s, 1H), 8.92 (s, 1H), 8.52 (s, 1H), 8.09 (d, *J* = 2.8 Hz, 1H), 7.96 (s, 1H), 7.76 (d, *J* = 8.8 Hz, 1H), 7.65 (d, *J* = 8.5 Hz, 2H), 7.41 (d, *J* = 6.6 Hz, 1H), 7.33 (s, 1H), 7.05 (d, *J* = 8.5 Hz, 2H), 4.12 (s, 3H), 4.04 (s, 2H), 2.66 (t, *J* = 5.8 Hz, 2H), 2.43 (s, 4H), 1.53–1.46 (m, 4H), 1.38 (d, *J* = 5.0 Hz, 2H).

(*E*)-*N*-(4-((4-chloro-3-fluorophenyl)amino)-7-methoxyquinazolin-6-yl)-2-(4-(2-morpholinoethoxy)benzylidene)hydrazine-1-carboxamide (**35**). This compound was obtained as white solid in 79% yield. Mp 210.2–215.3 °C. ESI-MS *m/z*: [M + H]<sup>+</sup> 593.20. <sup>1</sup>H NMR (400 MHz, DMSO-*d*<sub>6</sub>) δ 11.02 (s, 1H), 9.84 (s, 1H), 9.07 (s, 1H), 8.91

(s, 1H), 8.52 (s, 1H), 8.11 (s, 1H), 7.96 (s, 1H), 7.78 (s, 1H), 7.66 (d, *J* = 7.8 Hz, 2H), 7.45–7.38 (m, 1H), 7.33 (s, 1H), 7.06 (d, *J* = 8.0 Hz, 2H), 4.14 (s, 2H), 4.12 (s, 3H), 3.58 (s, 4H), 2.71 (s, 2H), 2.49–2.43 (m, 4H).

(*E*)-*N*-(4-((3-chloro-4-fluorophenyl)amino)-7-methoxyquinazolin-6-yl)-2-(4-(2-(4-methylpiperazin-1-yl)ethoxy)benzylidene)hydrazine-1-carboxamide (**36**). This compound was obtained as white solid in 91% yield. Mp 215.2–220.5 °C. ESI-MS *m/z*: [M + H]<sup>+</sup> 606.2. <sup>1</sup>H NMR (400 MHz, DMSO-*d*<sub>6</sub>) δ 10.99 (s, 1H), 9.80 (s, 1H), 9.01 (s, 1H), 8.86 (s, 1H), 8.46 (s, 1H), 8.04 (d, *J* = 4.9 Hz, 1H), 7.90 (s, 1H), 7.71 (s, 1H), 7.60 (d, *J* = 8.4 Hz, 2H), 7.36 (t, *J* = 9.3 Hz, 1H), 7.27 (s, 1H), 7.00 (d, *J* = 8.4 Hz, 2H), 4.07 (s, 2H), 4.05 (s, 3H), 2.68 (s, 2H), 2.44 (s, 8H), 2.28 (s, 3H).

(*S,E*)-*N*-(4-((3-chloro-4-fluorophenyl)amino)-7-((tetrahydrofuran-3-yl)oxy)quinazolin-6-yl)-2-(4-(2-(dimethylamino)ethoxy)benzylidene)hydrazine-1-carboxamide (**37**). This compound was obtained as white solid in 90% yield. Mp 221.5–231.8 °C. ESI-MS *m/z*: [M + H]<sup>+</sup> 607.2. <sup>1</sup>H NMR (400 MHz, DMSO-*d*<sub>6</sub>) δ 11.09 (s, 1H), 9.87 (s, 1H), 9.14 (s, 1H), 9.01 (s, 1H), 8.51 (s, 1H), 8.10 (s, 1H), 7.97 (s, 1H), 7.78 (s, 1H), 7.67 (d, *J* = 8.3 Hz, 2H), 7.42 (t, *J* = 9.1 Hz, 1H), 7.33 (s, 1H), 7.00 (d, *J* = 8.4 Hz, 2H), 5.45 (s, 1H), 4.10 (s, 2H), 4.04 (s, 2H), 3.98 (s, 1H), 3.89 (s, 1H), 2.63 (s, 2H), 2.22 (s, 6H), 2.18–2.13 (m, 2H).

(*S,E*)-*N*-(4-((3-chloro-4-fluorophenyl)amino)-7-((tetrahydrofuran-3-yl)oxy)quinazolin-6-yl)-2-(4-(2-(diethylamino)ethoxy)benzylidene)hydrazine-1-carboxamide (**38**). This compound was obtained as yellow solid in 89% yield. Mp 210.1–213.9 °C. ESI-MS *m/z*: [M + H]<sup>+</sup> 635.2. <sup>1</sup>H NMR (400 MHz, DMSO-*d*<sub>6</sub>) δ 11.10 (s, 1H), 9.87 (s, 1H), 9.14 (s, 1H), 9.01 (s, 1H), 8.51 (s, 1H), 8.09 (dd, *J* = 6.8, 2.3 Hz, 1H), 7.97 (s, 1H), 7.80–7.75 (m, 1H), 7.67 (d, *J* = 8.5 Hz, 2H), 7.41 (d, *J* = 9.1 Hz, 1H), 7.33 (s, 1H), 7.04–6.97 (m, 2H), 5.46 (s, 1H), 4.04 (s, 2H), 3.97 (d, *J* = 7.6 Hz, 2H), 3.88 (d, *J* = 4.4 Hz, 2H), 2.84 (s, 2H), 2.61 (s, 4H), 2.43 (dd, *J* = 13.8, 6.0 Hz, 1H), 2.20–2.12 (m, 1H), 1.00 (t, *J* = 6.7 Hz, 6H).

(*S,E*)-*N*-(4-((3-chloro-4-fluorophenyl)amino)-7-((tetrahydrofuran-3-yl)oxy)quinazolin-6-yl)-2-(4-(2-(pyrrolidin-1-yl)ethoxy)benzylidene)hydrazine-1-carboxamide (**39**). This compound was obtained as white solid in 88% yield. Mp 216.2–218.9 °C. ESI-MS *m/z*: [M + H]<sup>+</sup> 633.2. <sup>1</sup>H NMR (400 MHz, DMSO-*d*<sub>6</sub>) δ 11.07 (s, 1H), 9.86 (s, 1H), 9.14 (s, 1H), 9.01 (s, 1H), 8.50 (s, 1H), 8.09 (dd, *J* = 6.8, 2.4 Hz, 1H), 7.97 (s, 1H), 7.80–7.75 (m, 1H), 7.67 (d, *J* = 8.4 Hz, 2H), 7.40 (d, *J* = 9.2 Hz, 1H), 7.33 (s, 1H), 6.99 (d, *J* = 8.5 Hz, 2H), 5.45 (s, 1H), 4.09–4.02 (m, 4H), 3.96 (t, *J* = 7.8 Hz, 1H), 3.91–3.84 (m, 1H), 3.63–3.53 (m, 4H), 2.43 (t, *J* = 7.2 Hz, 2H), 2.37 (s, 4H), 2.16 (d, *J* = 7.2 Hz, 1H), 1.91–1.87 (m, 1H).

(*S,E*)-*N*-(4-((3-chloro-4-fluorophenyl)amino)-7-((tetrahydrofuran-3-yl)oxy)quinazolin-6-yl)-2-(4-(2-(piperidin-1-yl)ethoxy)benzylidene)hydrazine-1-carboxamide (**40**). This compound was obtained as yellow solid in 86% yield. Mp 213.4–218.4 °C. ESI-MS *m/z*: [M + H]<sup>+</sup> 647.2. <sup>1</sup>H NMR (400 MHz, DMSO-*d*<sub>6</sub>) δ 11.05 (s, 1H), 9.87 (s, 1H), 9.08 (s, 1H), 8.92 (s, 1H), 8.52 (s, 1H), 8.11 (d, *J* = 6.7 Hz, 1H), 7.96 (s, 1H), 7.78 (s, 1H), 7.66 (d, *J* = 8.4 Hz, 2H), 7.43 (t, *J* = 9.1 Hz, 1H), 7.33 (s, 1H), 7.06 (d, *J* = 8.5 Hz, 2H), 5.55 (s, 1H), 4.02–3.98 (m, 4H), 3.96–3.94 (t, *J* = 7.8 Hz, 1H), 3.91–3.84 (m, 1H), 2.89 (s, 2H), 2.53–2.48 (m, *J* = 7.2 Hz, 1H), 2.44 (s, 4H), 2.16–2.08 (m, *J* = 5.7 Hz, 1H), 1.50 (s, 4H), 1.39 (s, 2H).

(*S,E*)-*N*-(4-((3-chloro-4-fluorophenyl)amino)-7-((tetrahydrofuran-3-yl)oxy)quinazolin-6-yl)-2-(4-(2-morpholinoethoxy)benzylidene)hydrazine-1-carboxamide (**41**). This compound was obtained as white solid in 70% yield. Mp 214.2–216.5 °C. ESI-MS *m/z*: [M + H]<sup>+</sup> 649.2. <sup>1</sup>H NMR (400 MHz, DMSO-*d*<sub>6</sub>) δ 11.08 (s, 1H), 9.86 (s, 1H), 9.14 (s, 1H), 8.98 (d, *J* = 18.5 Hz, 1H), 8.50 (s, 1H), 8.09 (d, *J* = 7.0 Hz, 1H), 7.97 (s, 1H), 7.77 (d, *J* = 8.9 Hz, 1H), 7.67 (d, *J* = 8.4 Hz, 2H), 7.42 (t, *J* = 9.2 Hz, 1H), 7.33 (s, 1H), 7.01 (d, *J* = 8.4 Hz, 2H), 5.42

(d,  $J = 22.1$  Hz, 1H), 4.15 (d,  $J = 5.3$  Hz, 2H), 4.04 (s, 2H), 3.97 (d,  $J = 8.0$  Hz, 1H), 3.88 (d,  $J = 5.1$  Hz, 1H), 3.58 (s, 4H), 2.76–2.67 (m, 2H), 2.56–2.51 (m,  $J = 5.7$  Hz, 1H), 2.42 (d,  $J = 13.7$  Hz, 4H), 2.26–2.18 (m,  $J = 5.7$  Hz, 1H).

(*S,E*)-*N*-4-((3-chloro-4-fluorophenyl)amino)-7-((tetrahydrofuran-3-yl)oxy)quinazolin-6-yl)-2-(4-(2-(4-methylpiperazin-1-yl)ethoxy)benzylidene)hydrazine-1-carboxamide (**42**). This compound was obtained as white solid in 78% yield. Mp 206.210.2 °C. ESI-MS  $m/z$ :  $[M + H]^+$  662.2.  $^1\text{H}$  NMR (400 MHz, DMSO- $d_6$ )  $\delta$  11.08 (s, 1H), 9.86 (s, 1H), 9.14 (s, 1H), 8.98 (d,  $J = 18.5$  Hz, 1H), 8.50 (s, 1H), 8.09 (d,  $J = 7.0$  Hz, 1H), 7.97 (s, 1H), 7.77 (d,  $J = 8.9$  Hz, 1H), 7.67 (d,  $J = 8.4$  Hz, 2H), 7.42 (t,  $J = 9.2$  Hz, 1H), 7.33 (s, 1H), 7.01 (d,  $J = 8.4$  Hz, 2H), 5.42 (d,  $J = 22.1$  Hz, 1H), 4.15 (d,  $J = 5.3$  Hz, 2H), 4.04 (s, 2H), 3.97 (d,  $J = 8.0$  Hz, 1H), 3.88 (d,  $J = 5.1$  Hz, 1H), 3.58 (s, 4H), 2.76–2.67 (m, 2H), 2.58–2.56 (m,  $J = 5.7$  Hz, 1H), 2.42 (d,  $J = 13.7$  Hz, 4H), 2.35–2.08 (m, 2H), 2.21–2.18 (m,  $J = 5.7$  Hz, 1H).

(*E*)-*N*-4-((3-chloro-4-fluorophenyl)amino)-7-methoxyquinazolin-6-yl)-2-(4-(3-(dimethylamino)propoxy)benzylidene)hydrazine-1-carboxamide (**43**). This compound was obtained as yellow solid in 76% yield. Mp 209.3–213.5 °C. ESI-MS  $m/z$ :  $[M + H]^+$  565.2.  $^1\text{H}$  NMR (400 MHz, DMSO- $d_6$ )  $\delta$  11.10 (s, 1H), 9.93 (s, 1H), 9.16 (s, 1H), 9.01 (s, 1H), 8.61 (s, 1H), 8.19 (dd,  $J = 6.9, 2.7$  Hz, 1H), 8.06 (s, 1H), 7.88 (dt,  $J = 9.1, 3.4$  Hz, 1H), 7.74 (d,  $J = 8.1$  Hz, 2H), 7.51 (t,  $J = 9.2$  Hz, 1H), 7.42 (s, 1H), 7.13 (d,  $J = 8.3$  Hz, 2H), 4.21 (s, 3H), 4.14 (t,  $J = 6.4$  Hz, 2H), 2.46 (s, 2H), 2.24 (s, 6H), 2.01–1.93 (m, 2H).

(*E*)-*N*-4-((4-chloro-3-fluorophenyl)amino)-7-methoxyquinazolin-6-yl)-2-(4-(3-(diethylamino)propoxy)benzylidene)hydrazine-1-carboxamide (**44**). This compound was obtained as white solid in 79% yield. Mp 221.5–229.3 °C. ESI-MS  $m/z$ :  $[M + H]^+$  593.2.  $^1\text{H}$  NMR (400 MHz, DMSO- $d_6$ )  $\delta$  11.10 (s, 1H), 9.93 (s, 1H), 9.16 (s, 1H), 9.01 (s, 1H), 8.61 (s, 1H), 8.19 (dd,  $J = 6.9, 2.7$  Hz, 1H), 8.06 (s, 1H), 7.88 (dt,  $J = 9.1, 3.4$  Hz, 1H), 7.74 (d,  $J = 8.1$  Hz, 2H), 7.51 (t,  $J = 9.2$  Hz, 1H), 7.42 (s, 1H), 7.13 (d,  $J = 8.3$  Hz, 2H), 4.21 (s, 3H), 4.14 (t,  $J = 6.4$  Hz, 2H), 2.46 (s, 2H), 2.24 (s, 6H), 2.01–1.93 (m, 2H).

(*E*)-*N*-4-((3-chloro-4-fluorophenyl)amino)-7-methoxyquinazolin-6-yl)-2-(4-(3-(pyrrolidin-1-yl)propoxy)benzylidene)hydrazine-1-carboxamide (**45**). This compound was obtained as yellow solid in 77% yield. Mp 216.7–219.6 °C. ESI-MS  $m/z$ :  $[M + H]^+$  591.2.  $^1\text{H}$  NMR (400 MHz, DMSO- $d_6$ )  $\delta$  10.91–10.70 (m, 1H), 9.87 (s, 1H), 8.96 (s, 1H), 8.77 (s, 1H), 8.49 (s, 1H), 8.07 (s, 1H), 7.94 (s, 1H), 7.80–7.69 (m, 1H), 7.34 (d,  $J = 42.0$  Hz, 2H), 7.51 (t,  $J = 9.2$  Hz, 1H), 7.42 (s, 1H), 7.13 (d,  $J = 32.2$  Hz, 2H), 4.35 (s, 2H), 4.06 (s, 3H), 2.38–2.32 (m, 4H), 1.83 (s, 2H), 1.05 (t,  $J = 7.0$  Hz, 2H), 0.83 (t,  $J = 6.9$  Hz, 6H).

(*E*)-*N*-4-((3-chloro-4-fluorophenyl)amino)-7-methoxyquinazolin-6-yl)-2-(4-(3-(piperidin-1-yl)propoxy)benzylidene)hydrazine-1-carboxamide (**46**). This compound was obtained as white solid in 84% yield. Mp 218.5–221.5 °C. ESI-MS  $m/z$ :  $[M + H]^+$  605.2.  $^1\text{H}$  NMR (400 MHz, DMSO- $d_6$ )  $\delta$  11.02 (s, 1H), 9.85 (s, 1H), 9.06 (s, 1H), 8.92 (s, 1H), 8.52 (s, 1H), 8.10 (d,  $J = 6.9$  Hz, 1H), 7.96 (s, 1H), 7.77 (s, 1H), 7.65 (d,  $J = 8.7$  Hz, 2H), 7.42 (s, 1H), 7.33 (s, 1H), 7.04 (d,  $J = 8.7$  Hz, 2H), 4.12 (s, 3H), 4.05 (t,  $J = 6.2$  Hz, 2H), 2.38 (t,  $J = 6.7$  Hz, 2H), 2.33 (s, 4H), 1.91–1.87 (m, 2H), 1.48 (d,  $J = 4.9$  Hz, 4H), 1.37 (s, 2H).

(*E*)-*N*-4-((3-chloro-4-fluorophenyl)amino)-7-methoxyquinazolin-6-yl)-2-(4-(3-morpholinopropoxy)benzylidene)hydrazine-1-carboxamide (**47**). This compound was obtained as white solid in 79% yield. Mp 226.5–230.2 °C. ESI-MS  $m/z$ :  $[M + H]^+$  607.2.  $^1\text{H}$  NMR (400 MHz, DMSO- $d_6$ )  $\delta$  11.02 (s, 1H), 9.84 (s, 1H), 9.06 (s, 1H), 8.89 (d,  $J = 26.4$  Hz, 1H), 8.52 (s, 1H), 8.10 (d,  $J = 6.7$  Hz, 1H), 7.96 (s, 1H), 7.78 (s, 1H), 7.66 (d,  $J = 7.4$  Hz, 2H), 7.41 (dd,  $J = 18.2, 9.1$  Hz, 1H), 7.33 (s, 1H), 7.04 (d,  $J = 7.4$  Hz, 2H), 4.12 (s, 3H), 4.07 (d,  $J = 5.4$  Hz, 2H), 3.58 (s, 4H), 2.43 (t,  $J = 6.5$  Hz, 2H), 2.37 (s, 4H), 1.94–1.85 (m, 2H).

(*E*)-*N*-4-((3-chloro-4-fluorophenyl)amino)-7-methoxyquinazolin-6-yl)-2-(4-(3-(4-methylpiperazin-1-yl)propoxy)benzylidene)hydrazine-1-carboxamide (**48**). This compound was obtained as white solid in 88% yield. Mp 216.5–218.2 °C. ESI-MS  $m/z$ :  $[M + H]^+$  620.2.  $^1\text{H}$  NMR (400 MHz, DMSO- $d_6$ )  $\delta$  11.02 (s, 1H), 9.85 (s, 1H), 9.06 (s, 1H), 8.91 (s, 1H), 8.51 (s, 1H), 8.09 (d,  $J = 6.6$  Hz, 1H), 7.96 (s, 1H), 7.77 (s, 1H), 7.65 (d,  $J = 8.6$  Hz, 2H), 7.42 (t,  $J = 9.1$  Hz, 1H), 7.32 (s, 1H), 7.04 (d,  $J = 8.7$  Hz, 2H), 4.11 (s, 3H), 4.05 (s, 2H), 2.49–2.49 (m, 8H), 2.40 (d,  $J = 7.2$  Hz, 2H), 2.13 (s, 3H), 1.88 (d,  $J = 7.2$  Hz, 2H).

4-(*S,E*)-*N*-4-((3-chloro-4-fluorophenyl)amino)-7-((tetrahydrofuran-3-yl)oxy)quinazolin-6-yl)-2-(4-(3-(diethylamino)propoxy)benzylidene)hydrazine-1-carboxamide (**49**)/NMR (400 MHz, DMSO- $d_6$ )  $\delta$  11.08 (s, 1H), 9.86 (s, 1H), 9.13 (s, 1H), 9.00 (s, 1H), 8.50 (s, 1H), 8.08 (d,  $J = 6.9$  Hz, 1H), 7.98 (s, 1H), 7.78 (d,  $J = 10.0$  Hz, 1H), 7.66 (d,  $J = 8.4$  Hz, 2H), 7.41 (t,  $J = 9.1$  Hz, 1H), 7.32 (s, 1H), 6.98 (d,  $J = 8.5$  Hz, 2H), 5.44 (s, 1H), 4.04 (d,  $J = 4.8$  Hz, 4H), 3.96 (t,  $J = 7.6$  Hz, 1H), 3.89–3.85 (m, 1H), 2.44 (s, 1H), 2.37 (t,  $J = 7.1$  Hz, 2H), 2.27 (s, 1H), 2.15 (s, 6H), 1.85 (d,  $J = 6.8$  Hz, 2H).

(*S,E*)-*N*-4-((3-chloro-4-fluorophenyl)amino)-7-((tetrahydrofuran-3-yl)oxy)quinazolin-6-yl)-2-(4-(3-(diethylamino)propoxy)benzylidene)hydrazine-1-carboxamide (**50**). This compound was obtained as yellow solid in 86% yield. Mp 208.2–213.5 °C. ESI-MS  $m/z$ :  $[M + H]^+$  649.2.  $^1\text{H}$  NMR (400 MHz, DMSO- $d_6$ )  $\delta$  11.06 (s, 1H), 9.85 (s, 1H), 9.13 (s, 1H), 9.01 (s, 1H), 8.50 (s, 1H), 8.09 (dd,  $J = 6.9, 2.6$  Hz, 1H), 7.96 (d,  $J = 6.4$  Hz, 1H), 7.78 (dt,  $J = 8.8, 3.4$  Hz, 1H), 7.66 (d,  $J = 8.4$  Hz, 2H), 7.41 (t,  $J = 9.1$  Hz, 1H), 7.33 (s, 1H), 6.98 (d,  $J = 8.5$  Hz, 2H), 5.45 (s, 1H), 4.05 (dd,  $J = 8.3, 4.5$  Hz, 4H), 3.97 (q,  $J = 7.7$  Hz, 1H), 3.87 (td,  $J = 8.4, 4.5$  Hz, 1H), 2.54 (s, 2H), 2.46 (d,  $J = 7.0$  Hz, 4H), 2.43–2.36 (m, 1H), 2.20–2.11 (m, 1H), 1.83 (q,  $J = 6.7$  Hz, 2H), 0.94 (t,  $J = 7.1$  Hz, 6H).

(*S,E*)-*N*-4-((3-chloro-4-fluorophenyl)amino)-7-((tetrahydrofuran-3-yl)oxy)quinazolin-6-yl)-2-(4-(3-(pyrrolidin-1-yl)propoxy)benzylidene)hydrazine-1-carboxamide (**51**). This compound was obtained as white solid in 83% yield. Mp 223.1–230.5 °C. ESI-MS  $m/z$ :  $[M + H]^+$  647.2.  $^1\text{H}$  NMR (400 MHz, DMSO- $d_6$ )  $\delta$  11.08 (s, 1H), 9.87 (s, 1H), 9.14 (s, 1H), 9.00 (s, 1H), 8.50 (s, 1H), 8.08 (d,  $J = 4.8$  Hz, 1H), 7.96 (s, 1H), 7.77 (s, 1H), 7.66 (d,  $J = 8.5$  Hz, 2H), 7.41 (t,  $J = 9.0$  Hz, 1H), 7.32 (s, 1H), 6.98 (d,  $J = 8.3$  Hz, 2H), 5.45 (s, 1H), 4.04 (s, 4H), 3.96 (d,  $J = 7.7$  Hz, 1H), 3.87 (d,  $J = 4.3$  Hz, 1H), 2.53 (s, 2H), 2.43 (s, 4H), 2.14 (s, 2H), 1.93–1.85 (m, 2H), 1.68 (s, 4H).

(*S,E*)-*N*-4-((3-chloro-4-fluorophenyl)amino)-7-((tetrahydrofuran-3-yl)oxy)quinazolin-6-yl)-2-(4-(3-(piperidin-1-yl)propoxy)benzylidene)hydrazine-1-carboxamide (**52**). This compound was obtained as white solid in 81% yield. Mp 222.5–226.5 °C. ESI-MS  $m/z$ :  $[M + H]^+$  661.2.  $^1\text{H}$  NMR (400 MHz, DMSO- $d_6$ )  $\delta$  11.07 (s, 1H), 9.86 (s, 1H), 9.13 (s, 1H), 8.99 (s, 1H), 8.49 (s, 1H), 8.07 (dd,  $J = 6.9, 2.6$  Hz, 1H), 7.95 (s, 1H), 7.76 (s, 1H), 7.65 (d,  $J = 8.7$  Hz, 2H), 7.41 (t,  $J = 9.1$  Hz, 1H), 7.31 (s, 1H), 6.97 (d,  $J = 8.8$  Hz, 2H), 5.45 (s, 1H), 4.04 (d,  $J = 6.6$  Hz, 4H), 3.94 (s, 1H), 3.86 (d,  $J = 4.5$  Hz, 1H), 2.41–2.33 (m, 4H), 2.31 (s, 2H), 2.14 (s, 2H), 1.87 (d,  $J = 7.9$  Hz, 2H), 1.48 (s, 4H), 1.37 (s, 2H).

(*S,E*)-*N*-4-((3-chloro-4-fluorophenyl)amino)-7-((tetrahydrofuran-3-yl)oxy)quinazolin-6-yl)-2-(4-(3-morpholinopropoxy)benzylidene)hydrazine-1-carboxamide (**53**). This compound was obtained as white solid in 82% yield. Mp 226.5–229.5 °C. ESI-MS  $m/z$ :  $[M + H]^+$  663.2.  $^1\text{H}$  NMR (400 MHz, DMSO- $d_6$ )  $\delta$  10.97 (s, 1H), 9.84 (s, 1H), 9.10 (s, 1H), 8.98 (s, 1H), 8.43 (s, 1H), 8.03 (s, 1H), 7.95 (s, 1H), 7.70 (s, 1H), 7.65 (d,  $J = 8.4$  Hz, 2H), 7.36 (t,  $J = 9.1$  Hz, 1H), 7.26 (s, 1H), 6.97 (d,  $J = 8.4$  Hz, 2H), 5.41 (d,  $J = 8.2$  Hz, 1H), 4.06 (d,  $J = 6.2$  Hz, 2H), 4.02 (d,  $J = 3.4$  Hz, 2H), 3.94 (t,  $J = 7.7$  Hz, 1H), 3.87 (dd,  $J = 8.4, 4.7$  Hz, 1H), 3.56 (t,  $J = 4.6$  Hz, 4H), 2.43 (s, 1H), 2.41 (d,  $J = 7.1$  Hz, 2H), 2.35 (s, 4H), 2.14 (d,  $J = 8.8$  Hz, 1H), 1.90–1.84 (m, 2H).

(*S,E*)-*N*-(4-((3-chloro-4-fluorophenyl)amino)-7-((tetrahydrofuran-3-yl)oxy)quinazolin-6-yl)-2-(4-(3-(4-methylpiperazin-1-yl)propoxy)benzylidene)hydrazine-1-carboxamide (**54**). This compound was obtained as yellow solid in 81% yield. Mp 216.5–219.5 °C. ESI-MS *m/z*: [M + H]<sup>+</sup> 676.2. <sup>1</sup>H NMR (400 MHz, DMSO-*d*<sub>6</sub>) δ 11.07 (s, 1H), 9.85 (s, 1H), 9.12 (s, 1H), 8.99 (s, 1H), 8.48 (s, 1H), 8.06 (d, *J* = 7.1 Hz, 1H), 7.95 (s, 1H), 7.75 (s, 1H), 7.64 (d, *J* = 8.2 Hz, 2H), 7.40 (t, *J* = 9.0 Hz, 1H), 7.30 (s, 1H), 6.96 (d, *J* = 8.3 Hz, 2H), 5.43 (s, 1H), 4.13–4.00 (m, 4H), 3.95 (q, *J* = 7.5 Hz, 1H), 3.86 (dt, *J* = 12.2, 6.1 Hz, 1H), 2.60 (s, 2H), 2.45 (s, 1H), 2.43–2.35 (m, 4H), 2.35–2.22 (m, 4H), 2.15 (s, 1H), 2.12 (s, 3H), 1.96–1.77 (m, 2H).

## Biological evaluation

### Cytotoxicity assay *in vitro*

The cytotoxic activities of target compounds **9–54** were evaluated with HepG2, A549, MCF-7 and H1975 cell lines by the standard MTT assay *in vitro*, with compounds EGFR inhibitors afatinib as a positive control. The cancer cell lines were cultured in minimum essential medium (MEM) supplement with 10% fetal bovine serum (FBS). Approximately 4 × 10<sup>3</sup> cells, suspended in MEM medium, were plated onto each well of a 96-well plate and incubated in 5% CO<sub>2</sub> at 37 °C for 24 h. The test compounds at indicated final concentrations were added to the culture medium and the cell cultures were continued for 72 h. Fresh MTT was added to each well at a terminal concentration of 5 μg/mL and incubated with cells at 37 °C for 4 h. The formazan crystals were dissolved in 100 μL DMSO each well, and the absorbency at 492 nm (for absorbance of MTT formazan) and 630 nm (for the reference wavelength) was measured with the ELISA reader. All of the compounds were tested three times in each of the cell lines. The results expressed as inhibition rates or IC<sub>50</sub> (half-maximal inhibitory concentration) were the averages of two determinations and calculated by using the Bacus Laboratories Incorporated Slide Scanner (Bliss) software (Bacus Laboratories Inc, Lombard, IL, USA).

### EGFR kinases assay *in vitro*

The selected compounds with excellent anti-proliferative activities were tested for their activity against EGFR kinases through the mobility shift assay. All kinases assays were performed in 96-well plates in a 50 μL reaction volume. The kinase buffer contains 50 mM HEPES, pH 7.5, 10 mM MgCl<sub>2</sub>, 0.0015% Brij-35 and 2 mM DTT. The stop buffer contains 100 mM HEPES, pH 7.5, 0.015% Brij-35, 0.2% Coating Reagent #3 and 50 mM EDTA. The compounds were diluted to 500 μM by 100% DMSO, then 10 μL of compound was transferred to a new 96-well plate as the intermediate plate, and 90 μL kinase buffer was added to each well. Then 5 μL of each well of the intermediate plate was transferred to 384-well plates. The following amounts of enzyme and substrate were used per well: kinase base buffer, FAM-labeled peptide, ATP and enzyme solution. Wells containing the substrate, enzyme, DMSO without compound were used as DMSO control. Wells containing just the substrate without enzyme were used as a low control. Incubate at room temperature for 10 min. Add 10 μL peptide solution to each well. Incubate at 28 °C for specified period of time and stop reaction by 25 μL stop buffer. At last data was collected on Caliper program and conversion values were converted to inhibition values. Percent inhibition = (max – conversion)/(max – min) × 100. “max” stands for DMSO control; “min” stands for low control.

### Cell apoptosis assay by flow cytometry

A549 cells were seeded in 16-well plates at a density of 1 × 10<sup>6</sup> cells/well in RPMI 1640 medium and treated with 0.5, 1 μM **10d** for 48 h. Cultured cells were stained with Annexin V-FITC and propidium iodide (PI) in the dark at 4 °C for 30 min and analysed by FACS Calibur flow cytometer (Becton Dickinson, San Jose, CA) using Cell Quest software.

### Flow cytometric analysis of cell cycle distribution assay

For flow cytometric analysis of DNA content, 5.0 × 10<sup>5</sup> cell/well A549 cells were grown in a costar 6-well cell culture cluster and grown for 24 h at 37 °C in 5% CO<sub>2</sub>, after the medium was removed and the cells were treated with specific concentrations of the test compounds **14** and **44** for 48 h. Blank wells treated with medium only were also included. After the incubation period, the A549 cells were collected, washed twice with ice-cold PBS, centrifuged and then fixed with ice-cold ethanol (70%) for at least 24 h. Cells were then collected, washed twice with ice-cold PBS, and treated with 30 ml RNase A (1 mg/mL) in PBS at 37 °C for about 30 min, and then stained with 50 ml propidium iodide (50 mg/mL) in PBS, the staining process lasted 30 min at 4 °C in darkness. The cellular DNA content of the stained cells was then analysed on BD-FACS Aria III flow cytometer and the cell cycle distribution was quantified.

### Docking studies

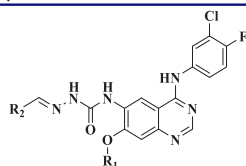
For docking purposes, the three-dimensional structure of the EGFR PDB code: 4G5P was obtained from RCSB Protein Data Bank. Autodock 4.2 (The Scripps Research Institute, La Jolla, CA, USA), Discover Studio 4.5 visualiser and Open Babel (Biovia Dassault System, Accelrys, San Diego, CA, USA) were used for the docking study. Firstly, using the Discover Studio 4.5 visualiser to prepare ligands (**14** and **44**) and acceptor protein (PDB code: 4G5P), then saved as pdb format after energy minimisation for ligand and clean protein, defined the activity site for acceptor protein. Secondly, the pdb file of ligand and the acceptor protein were converted to the pdbqt format by the Open Babel tool. Thirdly, docking was carried out by uploading the pdbqt file to the Autodock 4.5, and the result was named out.pdbq. Moreover, out.pdbqt file was uploaded to the Discover Studio 4.5 visualiser for analysing the result. All calculations were performed on Silicon Graphics workstation. Detailed user guidance and basic docking operations can be found on AutoDock official website <http://autodock.scripps.edu/faqs-help/tutorial>.

## Results and discussion

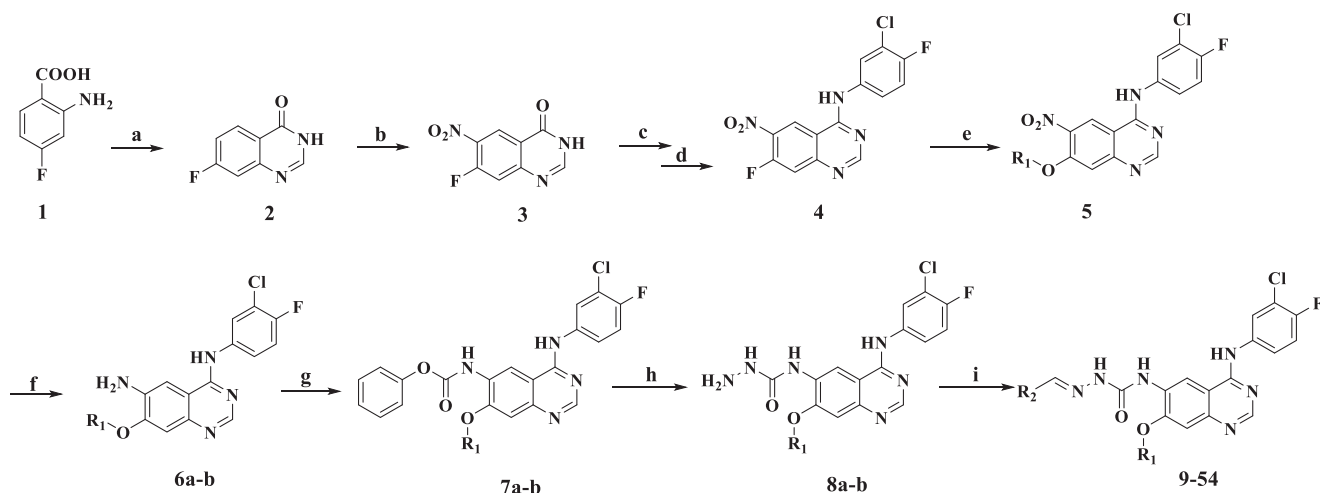
### Chemistry

The structure and synthetic route of **9–54** are shown by Table 1 and Scheme 1, respectively. The key intermediates **8a–b** was synthesised from commercially available 2-amino-4-fluorobenzoic acid through eight steps. Finally, condensation of **8a–b** with aromatic aldehydes in ethanol in the presence of a catalytic amount of glacial acetic acid yielded target compounds **9–54** respectively. Commercially available heterocyclic aldehydes reacted with **8a–b** produced compounds **9–18**, and side chains **57a–1** and **60a–f** reacted with **8a–b** produced compounds **18–54**.

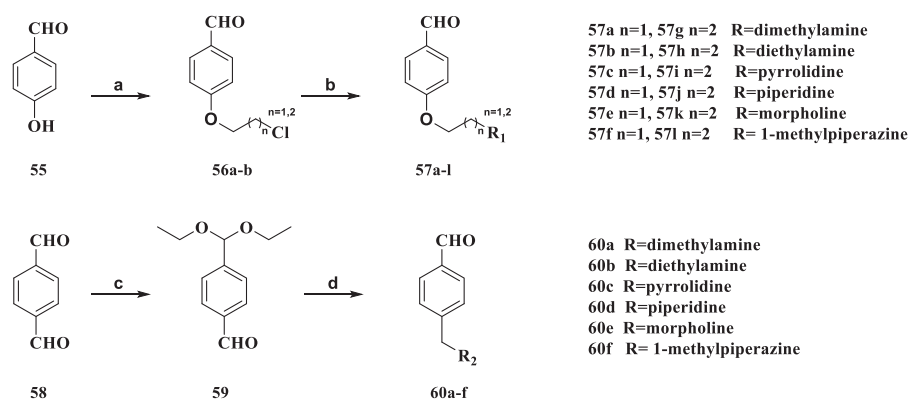
The general strategy for the synthesis of compounds **57a–1** and **60a–f** is shown in Scheme 2. The reaction of the commercially available 4-hydroxybenzaldehyde (**55**) with 1-bromo-2-chloroethane or 1-bromo-2-chloropropane produced intermediates

**Table 1.** Chemical structures of the target compounds 9–54.

Cpd. No	R <sub>1</sub>	R <sub>2</sub>	Yield (%)	Cpd. No	R <sub>1</sub>	R <sub>2</sub>	Yield (%)
9	Me		88	32	Me		79
10	Me		76	33	Me		84
11			86	34	Me		75
12			84	35	Me		79
13			86	36	Me		91
14			85	37			90
15			78	38			89
16			89	39			88
17	Me		77	40			86
18			79	41			70
19	Me		84	42			78
20	Me		86	43	Me		76
21	Me		89	44	Me		79
22	Me		92	45	Me		77
23	Me		87	46	Me		84
24	Me		81	47	Me		79
25			86	48	Me		88
26			81	49			81
27			83	50			86
28			87	51			83
29			86	52			81
30			85	53			82
31	Me		76	54			81



Scheme 1. Synthetic route of target compounds 9–54.



Scheme 2. Synthetic route of side chains 57a–l and 60a–f.

**56a–56b.** Nucleophilic aromatic substitution of the position of chlorine in **56a–58b** with small molecule amines in DMF at microwave 125 °C yielded compounds **57a–l**. Commercially available terephthalaldehyde (**58**) reacted with triethyl orthoformate to obtain the crude product and purified by column chromatography (PE/EA, 5.95v/v) to afford the intermediate **59**. Compound **59** was reductively aminated in the presence of sodium borohydride to give the crude product. Finally, a solution of the crude product in methanol reacted with a hydrochloric acid-methanol solution to afford the intermediate **60a–f**.

Reagents and conditions: (a) EtOH, Formamidinium acetate, 24h; (b) Con. $\text{H}_2\text{SO}_4$ , fuming  $\text{HNO}_3$ , 2h; (c)  $\text{SOCl}_2$ , DMF(cat.), 4h; (d) 3-chloro-4-fluoroaniline, Isopropanol, Triethylamine, 1.5h; (e) (S)-tetrahydrofuran-3-ol, 60% NaH, THF, 3h;  $\text{CH}_3\text{OH}$ , NaOH; (f) 80% hydrazine monohydrate,  $\text{FeCl}_3$ , activated carbon, EtOH, 1h; (g) phenyl chloroformate, DIPEA, 1,4-dioxane, 10 °C to rt, 1.5h; (h) 80% hydrazine monohydrate, 1,4-dioxane, reflux; (i) commercially available Heterocyclic aldehydes, acetic acid(Cat.), EtOH, reflux.

Reagents and conditions: (a) acetonitriles, anhydrous,  $\text{K}_2\text{CO}_3$ , 1-bromo-2-chloroethane or 1-bromo-2-chloropropane, 1 h, rt; (b) DMF, microwave, Small molecule amines, 1 h, rt. (c) triethyl orthoformate, ammonium chloride, r.t.; (d) 1, methanol water, sodium borohydride; 2, diluted hydrochloric acid, heated. 3, hydrogen chloride in methanol, T = 0–20 °C.

#### *In vitro* anti-proliferative activity screening of compounds 9–54

Taking afatinib as reference compound, the target compounds (**9–54**) were evaluated for the anti-proliferative activity against a

panel of four human cancer cell lines, belonging to different tumour types, namely human liver cancer cell lines (HepG2), human breast carcinoma cell lines (MCF-7), human lung carcinoma cell lines (A549), Human lung adenocarcinoma cell lines (H1975) at a concentration of 0.1–100 mM. HepG2, A549, and MCF-7 were selected to test the broad-spectrum anti-cell proliferative activity of compounds on tumour cells. H1975 was used to verify whether anti-cell proliferative activity was also observed for gefitinib-resistant cell lines. The results expressed as  $\text{IC}_{50}$  values were summarised in Table 2 and the values were the average of at least two independent experiments. The  $\text{IC}_{50}$  values that were higher than 100  $\mu\text{M}$  in all cell lines were not included.

As shown in Table 2, the results of the cells showed that after the C-7 position of the quinazoline nucleus was modified, the anti-proliferative activity of H1975 against most of the target compounds was significantly increased. However, compounds **23**, **24**, **29**, **38**, **39**, **43**, **49** were showed no activity on some cell lines. The potential compounds well inhibited the growth of H1975 cells with  $\text{IC}_{50}$  values ranging from  $0.83 \pm 0.17$  to  $16.58 \pm 1.39 \mu\text{M}$ . Notably, the anti-proliferative activity of compounds **14**, **28**, **44**, **46**, **50**, **52** and **54** against H1975 cells was a single-digit level with  $\text{IC}_{50}$  values of  $1.72 \pm 0.85$ ,  $3.97 \pm 0.64$ ,  $1.03 \pm 0.17$ ,  $3.10 \pm 0.49$ ,  $1.53 \pm 0.52$ ,  $2.20 \pm 0.37$  and  $6.23 \pm 0.99 \mu\text{M}$ , respectively. Likewise, compounds **10**, **12**, **13**, **19**, **21**, **24**, **37**, **42** and **48** showed moderate inhibitory activity. Unfortunately, compounds **9**, **15**, **16**, **20**, **25**, **32**, **34**, **36**, **38** and **49** had poorer cellular activity of H1975 despite their very good broad antitumour activity.

**Table 2.** *In vitro* anti-proliferative activities against different cancer cell lines for 72 h of the target compounds.

Cpd. No	Anti-proliferative activities in different cancer cell lines (IC <sub>50</sub> <sup>a</sup> , μM)			
	HepG <sub>2</sub>	A549	MCF-7	H1975
9	0.72 ± 0.19	2.84 ± 0.22	2.63 ± 0.16	40.72 ± 2.24
10	0.14 ± 0.08	1.51 ± 0.13	0.61 ± 0.12	12.32 ± 1.65
11	11.45 ± 1.16	31.4 ± 2.12	15.4 ± 1.14	40.27 ± 3.24
12	0.31 ± 0.13	0.28 ± 0.12	0.35 ± 0.09	10.59 ± 0.65
13	1.35 ± 0.31	1.48 ± 0.19	1.35 ± 0.14	16.32 ± 1.34
14	4.63 ± 0.36	5.9 ± 0.25	2.37 ± 0.34	1.72 ± 0.85
15	8.17 ± 0.98	10.51 ± 0.77	14.01 ± 0.78	32.27 ± 2.64
16	2.43 ± 0.45	2.5 ± 0.36	3.68 ± 0.49	60.27 ± 5.24
17	13.22 ± 1.31	14.56 ± 1.21	12.89 ± 1.12	35.26 ± 2.35
18	5.81 ± 0.61	19.2 ± 1.46	12.43 ± 1.25	51.59 ± 4.35
19	9.89 ± 0.96	7.99 ± 0.82	3.80 ± 0.22	15.65 ± 1.49
20	9.49 ± 0.47	8.71 ± 0.54	4.14 ± 0.57	76.27 ± 6.27
21	21.34 ± 1.47	17.82 ± 1.22	8.90 ± 0.48	16.58 ± 1.39
22	59.48 ± 4.75	24.22 ± 2.27	31.13 ± 2.55	63.35 ± 6.13
23	>100	>100	>100	>100
24	2.86 ± 0.13	4.32 ± 0.61	3.12 ± 0.38	15.26 ± 1.65
25	3.76 ± 0.21	4.13 ± 0.54	4.41 ± 0.28	40.27 ± 3.27
26	53.61 ± 4.75	23.14 ± 1.54	36.91 ± 3.54	62.57 ± 5.48
27	>100	>100	>100	>100
28	3.13 ± 0.45	2.25 ± 0.32	4.30 ± 0.63	3.97 ± 0.64
29	>100	>100	>100	65.24 ± 5.54
30	17.49 ± 1.62	24.95 ± 1.66	21.01 ± 1.68	36.27 ± 2.54
31	36.33 ± 2.57	40.12 ± 4.03	37.25 ± 2.89	45.27 ± 3.34
32	13.24 ± 1.03	8.62 ± 1.13	12.51 ± 1.24	32.56 ± 3.45
33	46.72 ± 4.46	36.42 ± 2.78	44.23 ± 3.75	49.27 ± 4.68
34	12.72 ± 1.25	10.85 ± 1.43	9.21 ± 1.16	61.57 ± 5.67
35	16.51 ± 1.42	19.54 ± 1.35	21.8 ± 1.34	25.17 ± 1.35
36	10.18 ± 1.09	11.38 ± 1.07	6.2 ± 0.81	24.65 ± 1.86
37	8.20 ± 0.81	14.66 ± 1.35	11.72 ± 1.34	10.16 ± 1.12
38	1.91 ± 0.34	3.01 ± 0.54	1.99 ± 0.68	>100
39	67.27 ± 6.24	63.86 ± 5.35	64.82 ± 5.35	>100
40	17.39 ± 1.24	24.22 ± 1.24	24.15 ± 1.23	35.28 ± 2.35
41	40.25 ± 3.04	37.76 ± 2.54	28.82 ± 1.29	25.47 ± 1.44
42	13.40 ± 0.54	2.52 ± 0.54	10.82 ± 0.68	11.17 ± 1.34
43	>100	43.07 ± 3.34	>100	>100
44	0.02 ± 0.01	0.41 ± 0.01	0.32 ± 0.02	1.03 ± 0.17
45	24.47 ± 1.27	23.19 ± 1.47	16.88 ± 1.34	38.24 ± 1.23
46	9.58 ± 0.94	4.01 ± 0.56	6.85 ± 0.65	3.10 ± 0.49
47	28.4 ± 1.78	34.82 ± 1.26	27.52 ± 1.29	41.23 ± 2.07
48	14.50 ± 1.27	2.96 ± 0.36	12.23 ± 0.89	10.17 ± 1.26
49	5.04 ± 0.64	9.48 ± 0.86	6.21 ± 0.68	32.83 ± 1.27
50	1.08 ± 0.17	1.11 ± 0.14	1.23 ± 0.37	1.53 ± 0.52
51	16.99 ± 1.04	33.84 ± 1.14	28.54 ± 1.27	18.56 ± 1.35
52	2.28 ± 0.26	4.65 ± 0.39	2.56 ± 0.46	2.20 ± 0.37
53	>100	>100	>100	24.83 ± 1.08
54	41.19 ± 2.04	39.99 ± 2.14	38.42 ± 1.26	6.23 ± 0.99
BMC201725-9o <sup>b</sup>	0.07 ± 0.61	1.32 ± 0.38	0.91 ± 0.29	>100
Afatinib <sup>b</sup>	1.40 ± 0.08	1.33 ± 0.09	2.63 ± 0.16	0.49 ± 0.08
Gefitinib <sup>b</sup>	/	2.17 ± 0.14	/	12.70 ± 2.98

The value ">100" indicates that no inhibitory effect at 100 μM compound concentration.

<sup>a</sup>The values are an average of two separate determinations.

<sup>b</sup>Used as a positive control.

Interestingly, compound **14** showed a slight selectivity for H1975 cells. It is noteworthy that compound **44** have inhibitory activity against H1975 cells with an IC<sub>50</sub> value of 1.03 ± 0.17 μM, which was lower than that of afatinib (0.49 ± 0.08 μM). However, the IC<sub>50</sub> values of other cells were 0.02 ± 0.01, 0.41 ± 0.01 and 0.32 ± 0.02 μM, respectively, which were slightly higher than that of afatinib (1.40 ± 0.83, 1.33 ± 1.28, 2.63 ± 1.06 μM).

### Structure-activity relationship analysis

In combination with the activity of all compounds on the four cells, we found that most of the compounds' activity is reduced in the b strategy. Affected by the 4 position of the aromatic ring, the density of the electron cloud of the aromatic ring is reduced. In strategy a, the cell activity of the three carbon chains is apparently stronger than that of the two carbons. Among them, compounds

**44** and **50** show the most prominent activity, they all have the characteristics of a tricarbon chain linker and diethylamine. In the c strategy, the activity on H1975 is significantly increased and the activity on other cells remained since the hydroxyl group is replaced by an amine, such as compounds **9–12**. When the aromatic ring is replaced with an aromatic heterocycle, the activity against all cells slightly decreases. Same as we expected, compounds **13** and **14** in which the aromatic rings contain two heteroatoms, exhibit very prominent inhibitory activity against H1975.

### Kinase inhibitory activity

In order to find inhibitors targeting L858R/T790M, some compounds with significant inhibitory activity against H1975 cells were selected. The *in vitro* enzymatic inhibitory activities against EGFR<sup>L858R/T790M</sup> and EGFR<sup>WT</sup> were evaluated by using the

**Table 3.** Inhibitory activity of selected compounds against different types of EGFRs *in vitro*.

Cpd. No	R <sub>1</sub>	R <sub>2</sub>	EGFR IC <sub>50</sub> (nM)		LogD <sub>7.4</sub> <sup>a</sup>
			WT	L858R/T790M	
10	Me		16.0	>1000	5.9
12			2.5	>1000	5.8
13			10.8	>1000	4.3
14			6.3	8.4	4.2
19	Me		2.1	508.4	3.7
21	Me		3.8	482.4	3.6
24	Me		4.0	>1000	4.2
28			4.0	>1000	4.1
37			1.2	248.1	3.4
42			2.3	213.5	4.1
44	Me		0.4	107.4	3.3
46	Me		1.9	320.5	4.0
48	Me		1.8	596.8	4.0
50			1.3	151.9	3.2
52			1.7	561.6	3.9
54			2.6	187.9	3.9
<b>BMC201725-90<sup>b</sup></b>	/	/	56	>1000	4.7
<b>Afatinib<sup>b</sup></b>	/	/	4.0	3.8	2.3
<b>Gefitinib<sup>b</sup></b>	/	/	3.25	823.7	2.5

The value ">1000" indicates that no inhibitory effect at 100 μM compound concentration.

<sup>a</sup>The result is predicted by <https://chemicalize.com/#/calculation>.

<sup>b</sup>Used as a positive control.

well-established ELISA-based assay, and afatinib was employed as positive controls (Table 3). Notably, compound **14** (IC<sub>50</sub> = 8.4 nM) with a 2-(pyrrolidin-1-yl) pyrimidine side chain at the 7-position of the quinazoline ring had almost the same inhibitory activity as

afatinib (IC<sub>50</sub> = 3.8 nM). Among the compounds tested, most of the compounds showed single-digit nanomolar levels of wild-type kinase activity. However, most compounds had low inhibitory activity against the L858R/T790M mutant. It is noteworthy that

when the C-7 side chain introduced a flexible hydrophobic chain, the inhibitory activity of these compounds on L858R/T790M kinase was significantly enhanced. Among them, compound **44** was the best representative. And the most potent compound **14** exhibited excellent inhibition against EGFR<sup>WT</sup> and EGFR<sup>L858R/T790M</sup> with an IC<sub>50</sub> at 6.3 nM and 8.4 nM, respectively.

#### Morphologic changes of A549 cells under inverted microscopy and fluorescence microscopy

To explain the inhibition of cell growth, the apoptotic experiment by acridine orange (AO) single staining would be carried out to exam the effect of compounds **14** and **44** on A549 cell. As shown in Figure 3, the control group cell (Figure 3(a)) was stained with

acridine orange (AO) and the shape of the cell was full and the edge was clear. But in the other pictures (Figure 3(b,c,d)), the cell showed an identical phenomenon, the shape of which was abnormal with cell shrinkage, chromatin condensation or decomposition into fragments of varying sizes. This phenomenon indicated that compounds **14** and **44** can induce A549 cell apoptosis.

#### Induction of apoptosis assay on A549 cells

Apoptosis refers to the autonomous and orderly death of cells controlled by genes. Furthermore, its startup is affected by many external factors. To further elucidate the relationship between apoptosis and compounds **14** and **44**, Annexin V-FITC and propidium iodide (PI) double staining flow cytometry was used to

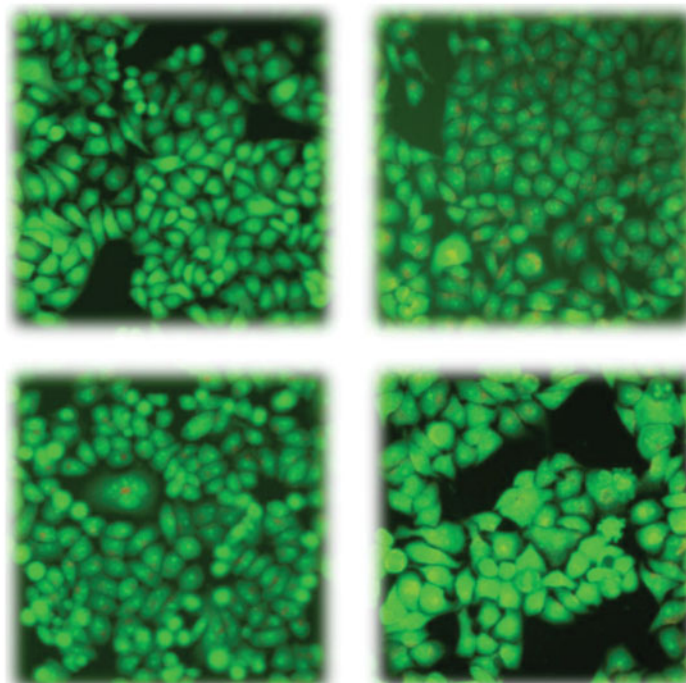


**Figure 3.** Morphologic changes of A549 cells under inverted microscopy and fluorescence microscopy. 3(a) the control group cell treated with nothing; 3(b) Experimental group treated with 1.33  $\mu\text{M}$  concentration of afatinib. 3(c) Experimental group treated with 1.59  $\mu\text{M}$  concentration of **14**. 3(d) Experimental group treated with 0.41  $\mu\text{M}$  concentration of **44**.

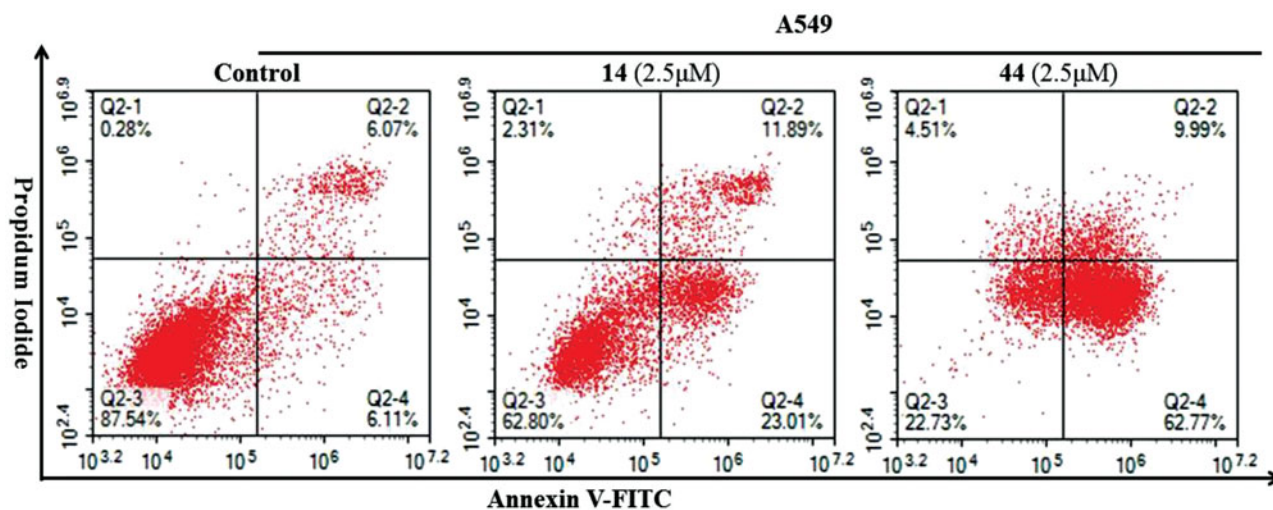


**Figure 4.** Cell apoptosis analysis on A549 cells treated with compounds **14** and **44** at 2.5  $\mu\text{M}$  detected by FCM.

evaluate the effect of compounds **14** and **44** on apoptosis of A549 cells at specific concentrations influences. The results are shown in Figure 4.

According to the results of Figure 4, compounds **14** and **44** effectively induced cell apoptosis at a concentration of 2.5  $\mu$ M. Treatment of A549 cells with compounds **14** and **44** for 48 h resulted in 34.9% and 72.76% of apoptotic cells (early+late), respectively, compared to 12.18% of apoptotic cells in the untreated control. These results revealed that compounds **14** and **44** inhibited cell growth through cell apoptosis induction.

#### Cell cycle analysis on A549 cells by flow cytometry

Aiming to better elucidate the relationship between the mechanism of inhibition of proliferation and cell cycle arrest, cells cycle distribution on A549 cells by treating with 2.5  $\mu$ M concentrations compounds **14** and **44** were performed. The results are shown in Table 4 and Figure 5. The region marked with different colours represents % population at different phases of the cell cycle. As can be seen, compound **14** caused an increase in the proportion of cells in S phase (from 40.03% in the control to 50.68%) with a concomitant decrease of cells in G0/G1 phase of the cell cycle (from 26.57% in the control to 23.62%) and cells in G2/M phase of the cell cycle (from 29.4% in the control to 25.7%). Interestingly, the effects of compound **44** and compound **14** on cell cycle were quite different. As shown in Figure 5, compound **44** caused an increase in the proportion of cells that cause G0/G1 phase cells (from 26.57% to 50.01% of controls), accompanied the decrease of S phase cell ratio (23.62% from 26.57% of controls) and G2/M phase cell ratio (from 29.4% in the control group to 25.7%). These results indicated that compounds **14** and **44** can inhibit tumour cell proliferation and lead to apoptosis by blocking the cell cycle.

**Table 4.** Analysis of cell cycle on A549 cells treated at 25  $\mu$ M compound 14 and 44 for 48 h by flow cytometry.

Cpd. No	G0/G1 (%)	S (%)	G2/M (%)	CV G1 (%)	CV G2 (%)
DMSO	26.57	44.03	29.40	3.71	3.83
14	23.62	50.68	25.70	3.34	5.15
44	50.10	31.91	17.99	3.94	3.48

#### Molecular docking study

To better understand how the **14** and **44** contributed to the EGFR kinase inhibitory activities, molecular docking simulation studies were carried out by using AutoDock 4.2, Open Babel and Discover Studio 4.5 visualizer. And based on the *in vitro* inhibition results, we selected compounds **14** and **44**, our best EGFR inhibitors in this study, as the ligand examples. And the co-crystal structure of EGFR<sup>T790M</sup> in complex with afatinib was obtained from the RSC Protein Data Bank (PDB code: 4G5P). The four selected compounds (afatinib, **BMC201725-9o**, **14** and **44**) occupied the ATP site of EGFR kinase (Figure 6(a)). The binding patterns of compounds **14** and **44** to EGFR kinase are shown in detail in Figure 6(b,c,d).

As clearly shown in Figure 6(b), the two compounds **14** and **44** all formed a hydrogen bond from the N1 of quinazoline core to the main chain NH of Met793, and the length of hydrogen bond were 2.0 and 2.3 Å, respectively. Compared to afatinib and **44**, another hydrogen bond existed between **44** and EGFR from NH in the Hydrazine carboxamide of **44** to the residue Asp800 of EGFR with the length of 2.1 Å (Figure 6(b)). Furthermore, several interactions existed between **14** and the residues of protein, such as pi-Alkyl interactions of the 3-Chloro-4-fluoroaniline with Met790 and Lys745. Alkyl interactions of the quinazoline ring with Leu718 and Ala743. There was a hydrogen-carbon interaction between the pyrimidine ring and Asp800 (Figure 6(c)). Interestingly, compound **44** had pi-sigma interactions between its hydrophobic side-chain ends and Phe723 in addition to the above several interactions (Figure 6(d)). These all indicated that the introduction of Heterocyclic aldehydes and flexible hydrophobic side chains to C-7 of TYB-65 led to a new binding interaction with the EGFR-TK domain, which contributed to its inhibitory activity against EGFR.

#### Conclusion

Herein, we used three different modification methods to structurally modify our previously studied compound **BMC201725-9o**, which led to the design and synthesis of a series of new derivatives and increased activity on EGFR<sup>L858R/T790M</sup>. These compounds were subjected to biological activities evaluation including anti-proliferative effects against four tumour cell lines (HepG2, A549, MCF-7 and H1975). Most of the synthesised compounds exhibited moderate to excellent anti-proliferative activities against the

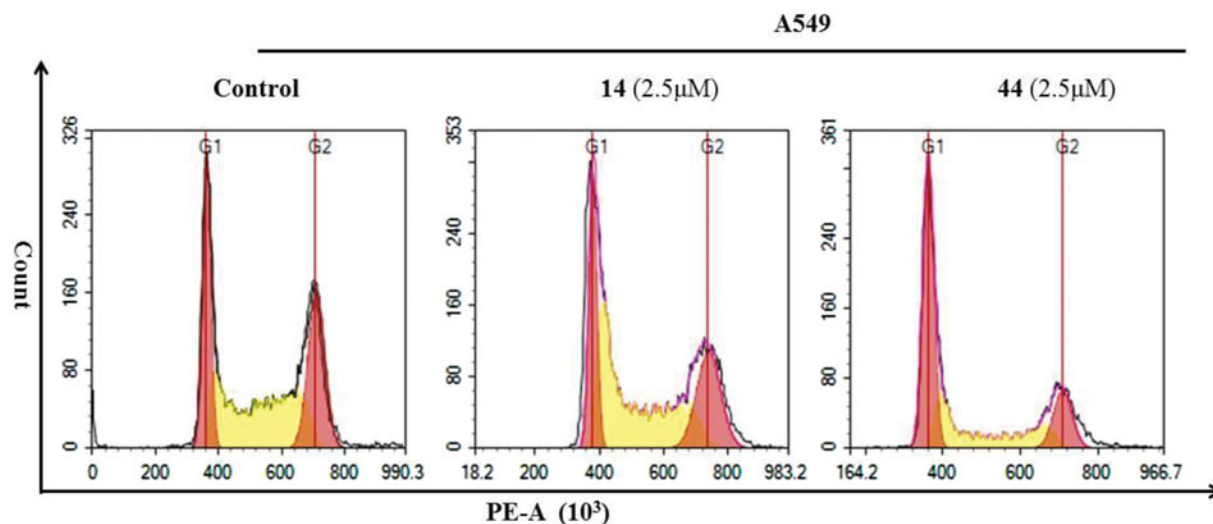


**Figure 5.** Cell cycle distribution of A549 cells treated at 2.5  $\mu$ M compound 14 and 44 for 48 h detected by FCM.

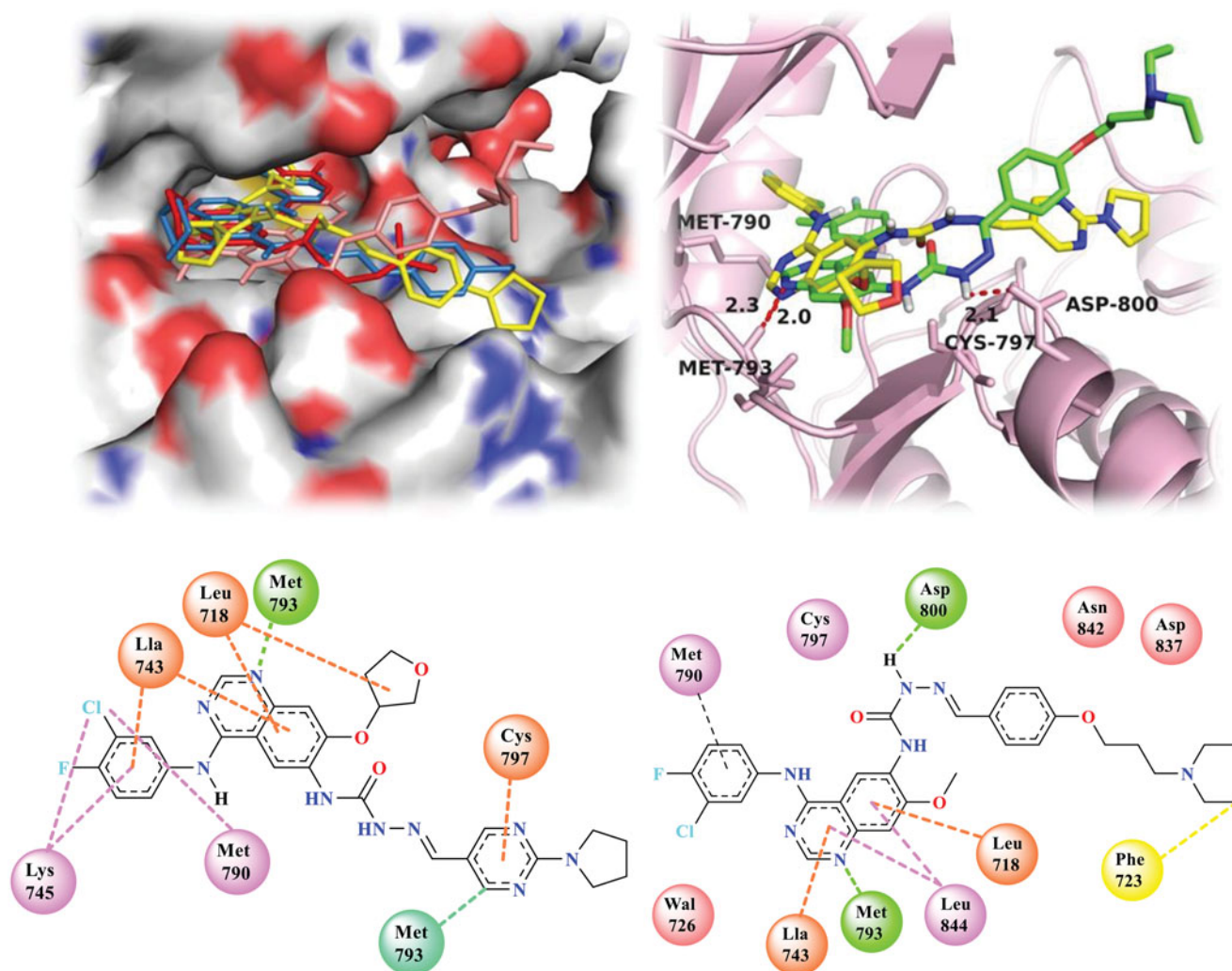


**Figure 6.** The protonated state of several important residue were adjusted by using AutoDock 4.5 in favour of forming reasonable hydrogen bond with the ligand and Molecular docking analysis was carried out by the Discover Studio 4.5 visualizer to explore the binding model for the active site of EGFR with its ligand. Docking simulations showed that the four selected compounds (afatinib, BMC201725-9o, **14** and **44**) occupied the ATP site of EGFR kinase 6(a). Then we employed 3D interaction map 6(b), 2D diagram of the compound **14** 6(c) and 2D diagram of the compound **44** 6(d) to display the interaction with the targeted protein (4G5P).

tested tumour cell lines. The hit **44** exhibited excellent inhibition of the tested tumour cell lines with the  $IC_{50}$  values of  $0.02 \pm 0.01 \mu M$ ,  $0.41 \pm 0.013 \mu M$ ,  $0.32 \pm 0.02 \mu M$  and  $0.83 \pm 0.17 \mu M$ , respectively. An EGFR kinase inhibition assay indicated that some of the tested derivatives displayed good inhibition against EGFR<sup>WT</sup> and EGFR<sup>L858R/T790M</sup>. Notably, compound **14** not only exhibited excellent anti-proliferative activity against the tumour cells, but also showed potent inhibitory activity toward EGFR<sup>WT</sup> ( $IC_{50}$  6.3 nM) and EGFR<sup>L858R/T790M</sup> ( $IC_{50}$  8.4 nM), similar to that of afatinib ( $IC_{50}$  4.0 and 3.8 nM). According to the result of AO single staining and Annexin V/PI staining, the **14** and **44** could induce remarkable apoptosis of A549 cells. Compound **14** caused S phase arrest and induced apoptosis to inhibit cell proliferation. Compound **44**, on the other hand, caused arrest in G0/G1 phase to induce apoptosis. In general, compounds **14** and **44** exerted potential antitumour activity through several mechanisms, including anti-proliferation and cell cycle arrest, and may serve as model molecule to help us to further design and develop more potent anticancer agents. These findings presented herein show the noncovalent inhibitor **14** and **44** have the potential to target EGFR mutants. The results also provide more insights for designing new classes of mutant-selective EGFR inhibitors.

## Disclosure statement

No potential conflict of interest was reported by the authors.

## Funding

This work was supported by The National Natural Science Funds of China [No. 21662014, 81460527], Outstanding Youth Foundation of Jiangxi, Natural Science Foundation of Jiangxi, China [20171BCB23078], Natural Science Foundation of Jiangxi, China [20171ACB21052 & 20171BAB215073].

## References

1. Song Z, Ge Y, Wang C, et al. Challenges and perspectives on the development of small-molecule EGFR inhibitors against T790M-mediated resistance in non-small-cell lung cancer. *J. Med. Chem* 2016;59:6580–94.
2. Zhang H-Q, Gong F-H, Ye J-Q, et al. Design and discovery of 4-anilinoquinazoline-urea derivatives as dual TK inhibitors of EGFR and VEGFR-2. *Eur J Med Chem* 2017;125: 245–54.

3. Han J, Henriksen S, Nørsett KG, et al. Balancing potency, metabolic stability and permeability in pyrrolopyrimidine-based EGFR inhibitors. *Eur J Med Chem* 2016;124:583–607.
4. Amin KM, Barsoum FF, Awadallah FM, et al. Identification of new potent phthalazine derivatives with VEGFR-2 and EGFR kinase inhibitory activity. *Eur J Med Chem* 2016;123:191–201.
5. Chen L, Fu W, Feng C, et al. Structure-based design and synthesis of 2,4-diaminopyrimidines as EGFR L858R/T790M selective inhibitors for NSCLC. *Eur J Med Chem* 2017;140:510–27.
6. Kobayashi S, Boggon TJ, Dayaram T, et al. EGFR mutation and resistance of non-small-cell lung cancer to gefitinib. *N Engl J Med* 2005;352:786–92.
7. Engelman JA, Jänne PA. Mechanisms of acquired resistance to epidermal growth factor receptor tyrosine kinase inhibitors in non-small cell lung cancer. *Clin Cancer Res* 2008;14:2895–9.
8. Ou SHI. Second-generation irreversible epidermal growth factor receptor (EGFR) tyrosine kinase inhibitors (TKIs): a better mousetrap? A review of the clinical evidence. *Crit Rev Oncol Hematol* 2012;83:407–21.
9. Ward RA, Anderton MJ, Ashton S, et al. Structure- and reactivity-based development of covalent inhibitors of the activating and gatekeeper mutant forms of the epidermal growth factor receptor (EGFR). *J Med Chem* 2013;56:7025–48.
10. Liu Q, Sabnis Y, Zhao Z, et al. Developing irreversible inhibitors of the protein kinase cysteinome. *Chem Biol* 2013;20:146–59.
11. Zhou W, Ercan D, Chen L, et al. Novel mutant-selective EGFR kinase inhibitors against EGFR T790M. *Nature* 2009;462:1070–4.
12. Thress KS, Paweletz CP, Felip E, et al. Acquired EGFR C797S mutation mediates resistance to AZD9291 in non-small cell lung cancer harboring EGFR T790M. *Nature Med* 2015;21:560.
13. Bryan MC, Burdick DJ, Chan BK, et al. Pyridones as highly selective, noncovalent inhibitors of T790M double mutants of EGFR. *ACS Med Chem Lett* 2016;7:100–4.
14. Heald R, Bowman KK, Bryan MC, et al. Noncovalent mutant selective epidermal growth factor receptor inhibitors: a lead optimization case study. *J Med Chem* 2015;58:8877–95.
15. Shao J, Chen E, Shu K, et al. 6-Oxooxazolidine-quinazolines as noncovalent inhibitors with the potential to target mutant forms of EGFR. *Bioorg Med Chem* 2016;24:3359–70.
16. Tu Y, Wang C, Xu S, et al. Design, synthesis, and docking studies of quinazoline analogues bearing aryl semicarbazone scaffolds as potent EGFR inhibitors. *Bioorg Med Chem* 2017;25:3148–57.